THESIS FOR THE DEGREE OF DOCTOR OF PHILISOPHY

Interrogation of drug effects on the lipid composition of single cells and *Drosophila* brain using ToF-SIMS imaging

Thuy Mai Hoang Philipsen

Department of Chemistry and Chemical Engineering

Chalmers University of Technology

Gothenburg, Sweden

2020

Interrogation of drug effects on the lipid composition of single cells and *Drosophila* brain using ToF-SIMS imaging

Thuy Mai Hoang Philipsen

Department of Chemistry and Chemical Engineering
Chalmers University of Technology
SE-412 96 Gothenburg
Sweden
Telephone: +46 (0)31 772 1000

Cover: A schematic of time-of-flight secondary ion mass spectrometry illustrates the ionization process where a primary ion beam bombards the sample surface to generate secondary ions.

Interrogation of drug effects on the lipid composition of single cells and *Drosophila* brain using ToF-SIMS imaging

Thuy Mai Hoang Philipsen
Department of Chemistry and Chemical Engineering
Chalmers University of Technology, Gothenburg, Sweden 2020

ABSTRACT

Lipids are essential for all living organisms on Earth. The most important function of lipids is that they act as the building blocks of cellular membranes. Lipids consist of polar head groups and non-polar tail groups and assemble into bilayer structures to create cell and organelle membranes. The plasma membrane of a cell provides a barrier which segregates cellular internal constituents from the external environment. In addition to acting as a barrier, membrane lipids are involved in many cellular processes including membrane trafficking, signal transduction, fission and fusion. Therefore, various conditions in the central nervous system involving lipid deficiencies can lead to function deficit. There are several drugs that induce the dysregulation of lipid metabolism linked to the impairment or enhancement of cognitive function. Hence, I have studied the lipid alterations in brain induced by drugs with regards to their effects on cognitive processes: cognitive impairing drugs (cocaine and zinc deficiency) and cognitive enhancing drugs (methylphenidate and fatty acids). Much work has been done to investigate the link between lipid metabolisms and these drugs. A powerful technique for lipid analysis is mass spectrometry imaging (MSI). MSI is a surface sensitive method which enables label-free detection of molecules in complex biological systems. In addition, MSI provides the relative composition as well as allows imaging of intact species with high spatial resolution in single experiments. One of the most common MSI techniques is time-of-flight secondary ion mass spectrometry (ToF-SIMS), which achieves high spatial resolution using a focused ion beam to eject and ionize molecules in the sample surface. Recently, gas cluster ion beams have been introduced to reduce the chemical damage during sampling of surfaces and to achieve enhancement of lipid signals. In our studies, ToF-SIMS has been applied to lipids in the membranes of cells and *Drosophila melanogaster* brain to get a better understanding about the effect of drugs in lipid mechanisms related to neuronal signal transmission.

The papers included in this thesis describe the application of ToF-SIMS in biological samples to reveal the alterations of lipids after drug treatments. In paper I, the alterations in lipid distribution and composition induced by cocaine and methylphenidate, which cause the impairment and enhancement in cognitive performance respectively, were investigated. ToF-SIMS data were used to show that cocaine and methylphenidate have opposite effects on the relative levels of lipids in the central fly brain. To enhance our understanding about the lipid mechanisms, in paper II, I used stable deuterium-labeled omega-3 and -6 fatty acids as lipid precursors to analyze the synthesis and transportation of lipids into the plasma membrane of PC12 cells. The use of isotope-labeled fatty acids provided a tool to track the lipid turn-over as well as to measure their relative amounts. Paper III continued the work done in paper I, where experiments were performed to investigate the recovery of lipids after cocaine removal. In addition, the cognitive-enhancing drug, methylphenidate, was used to treat cocaine removal from flies to investigate the reversal of lipid changes in the brain caused by repeated-cocaine exposure. Zinc deficiency in the diet, which causes a decrease in cognitive function, was also studied in fly brain. ToF-SIMS data obtained reveal that the lipid types that change are similar to those when treated with cocaine as seen in paper IV.

ToF-SIMS opens a new approach to visualize and relatively quantify phospholipids in biological tissues and cells. In the biological model systems studied here, cognition-affecting drugs show that alterations in the distribution and composition of specific lipids is altered differently based on whether the drug enhances versus diminishes cognition. These results provide new possible targets for lipid-modifying therapies to improve the cognitive decline in drug abuse and diseases.

Keywords: Mass spectrometry imaging, ToF-SIMS, lipid change, cognition, cocaine, methylphenidate, omega-3 and 6- fatty acids, zinc deficiency, Drosophila melanogaster, PC12 cell.

List of publications and contribution report

The thesis is based on the following publications.

I. Mass spectrometry imaging shows cocaine and methylphenidate have opposite effects on major lipids in *Drosophila* brain
Hoang Philipsen, M., Phan, T.N.N., Malmberg, P., Fletcher, J., Ewing, A. *ACS Chem. Neurosci.*, 2018, 9(6),1462-1468

Participated in designing and performing experiments together with N. Phan. Responsible for analysing and interpreting the data, as well as writing and editing the manuscript with other authors.

II. Relative quantification of deuterated omega-3 and -6 fatty acids and their lipid turnover in PC12 cell membranes using ToF-SIMS
Hoang Philipsen, M., Sämfors, S., Malmberg, P., Ewing, A. *Journal of Lipid Research*, 2018, 59, 2098-2107

Performed sample preparation for mass spectrometry imaging experiment. Analyzed and discussed data with co-authors. Participated in writing and editing the manuscript.

III. The interplay between cocaine, drug removal and methylphenidate rescue on phospholipid alterations in *Drosophila* brain determined by imaging mass spectrometry
Hoang Philipsen, M., Phan, T.N.N., Fletcher, J.S., Ewing, A. *ACS Chem. Neurosci.*, 2020, 11(5), 806-813

Contributed to planning and designing the project with N. Phan. Performed sample preparation, analyses, interpreted the data, as well as discussed the results with co-author. Participated in writing and editing the manuscript.

IV. Imaging mass spectrometry shows that zinc deficiency leads to lipid changes in *Drosophila* brain similar to cognitive impairing drugs
Hoang Philipsen, M.,[§] Gu, C.,[§] Ewing, A. *Submitted*

Performed mass spectrometry imaging experiments, analyzed, interpreted and discussed the data with co-authors. Wrote the first draft of the manuscript and edited the manuscript with C. Gu and A. Ewing.

[§] *The authors contributed equally to the work.*

Related publications not included in the thesis

Electrochemistry in and of the fly brain

Majdi, S., Larsson, A., Hoang Philipsen, M. *Electroanalysis*, 2018, 30, 999-1010

Effect of omega-3 and -6 fatty acids on exocytosis, vesicle content and lipid composition in PC12 cells

Gu, C., Hoang Philipsen, M., Ewing, A. Manuscript in preparation

Correlating between cellular membrane lipid alteration and activity-induced plasticity in exocytosis

Hoang Philipsen, M.,[§] Gu, C.,[§] Ewing, A. Manuscript in preparation

Screening of ^{13}C labelled distribution in freeze dried PC12 cells with ToF-SIMS

Hoang Philipsen, M.,[§] Penen, F.,[§] Ewing, A., Malmberg, P. Manuscript in preparation

[§] *The authors contributed equally to the work.*

Table of contents

Abbreviations

ER	Endoplasmic reticulum
FA	Fatty acid
MUFA	Monounsaturated fatty acid
PUFA	Polyunsaturated fatty acid
TAG	Triacylglycerol
DAG	Diacylglycerols
MAG	Monoacylglycerols
PA	Phosphatidic acid
PC	Phosphatidylcholines
CDP	Cytidine diphosphocholine
PE	Phosphatidylethanolamine
PI	Phosphatidylinositol
PIP	Phosphoinositide
PI(4)P	Phosphatidylinositol 4-phosphate
PI(4,5)P$_2$	Phosphatidylinositol 4,5-biphosphate
PS	Phosphatidylserine
PG	Phosphatidylglycerol
CL	Cardiolipin
SM	Sphingomyelin
MSI	Mass spectrometry imaging
SIMS	Secondary ion mass spectrometry
ToF	Time-of-flight
ToF-SIMS	Time-of-flight SIMS
MS	Mass spectrometry
MALDI	Matrix-assisted laser desorption/ionization
ESI	Electrospray ionization
DESI	Desorption electrospray ionization

FT-ICR	Fourier-transform ion cyclotron resonance
GCIB	Gas cluster ion beam
LMIG	Liquid metal ion gun
PC12 cell	Pheochromocytoma cell
MVA	Multivariate analysis
PCA	Principal components analysis
PC1	First principal component
MPH	Methylphenidate

Chapter 1

Cellular communication

Cells do not behave as isolated entities but tend to form complex networks that require cell-to-cell communication. Cell-to-cell communication is an essential process which helps cells to respond and adapt with environmental modifications, such as nutrients, and variation in temperature or light levels. Malfunction in cellular communication promotes development of various pathologies including cancer and degenerative diseases. Therefore, understanding of molecular basic for cell-to-cell communication provides new opportunities to develop new therapies to treat diseases resulting from improper signaling. This chapter introduces how signals can pass from one cell to another. Additionally, the effects of psychostimulants on signal transduction are also described together with neuroscientific approaches to the study of these effects.

1.1 The nerve cell is a core component in the activity of the nervous system

The human brain is made up of the nervous system, which is a complex network of millions nerve cells known as neurons. Although neurons have different morphologies and functions, they all contain four regions: the cell body, dendrites, axon and axon terminals (Figure 1.1). Each region has a specific function in communicating with other neurons.
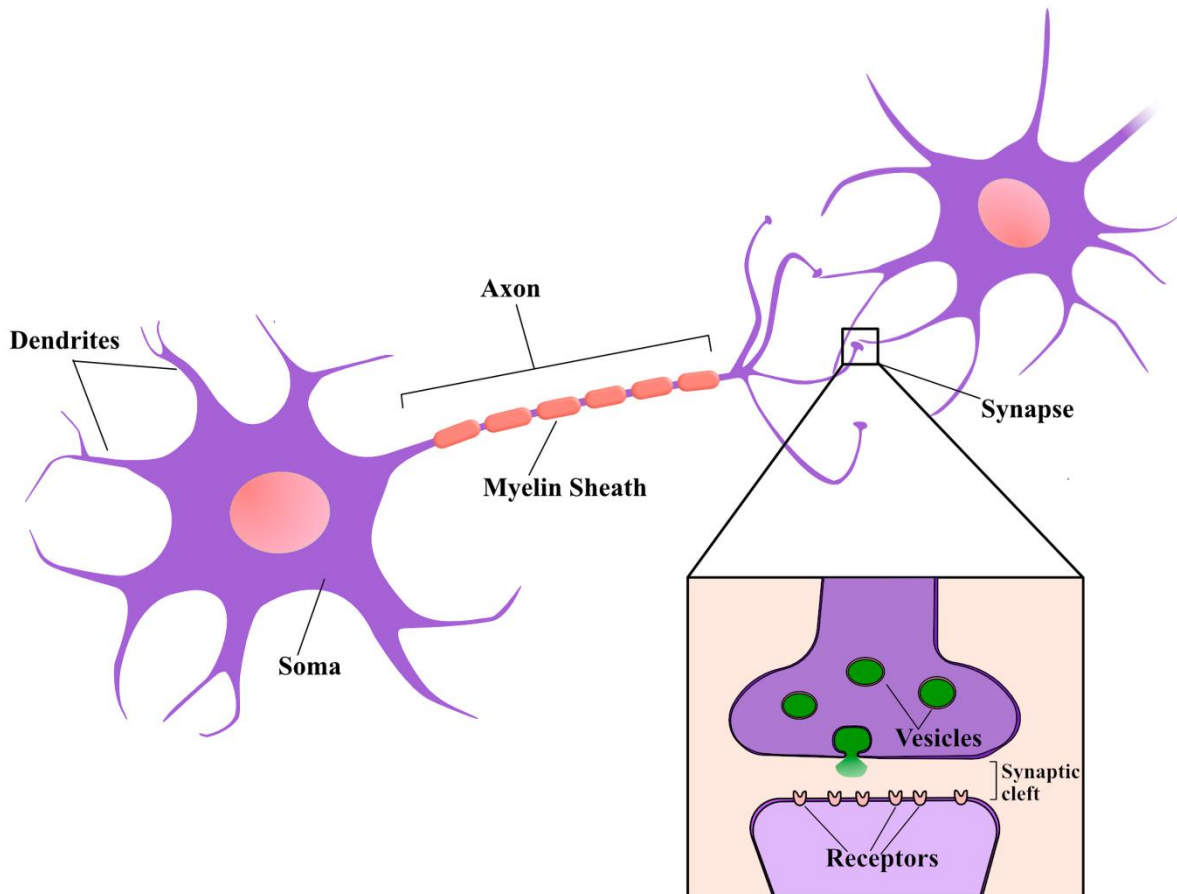
Figure 1.1. The structure of a typical neuron including cell body, dendrites, axon, and axon terminal. The synapse is a specific site where neurons communicate with each other. The space between an axon terminal and a dendrite of a receiving neuron is known as the synaptic cleft. This image is modified from Fischbach *et al.*[1]

In order to form a network, neurons connect with other neurons via special parts called dendrites. Dendrites are branched extensions from the cell body and are responsible for receiving signals from neighboring neurons. Neurons store their genetic information in the nucleus located in the cell body, also known as the soma. In addition to the nucleus, the soma contains major cytoplasmic organelles, such as mitochondria, Golgi apparatus, and endoplasmic reticulum (ER). The soma is mainly responsible for the synthesis of all proteins, which are then transported to their appropriate areas within neurons via axonal microtubules. Leading out of the cell body is a long and thin fiber called an axon that carries nerve impulses, or action potentials, away from the soma to other neurons. Myelin sheaths are wrapped around the nerve axon to speed up the propagation of action potentials along the axon. The end of the axon separates into several terminals which serve to pass the action potentials to adjacent neurons. The nerve terminal contacts with the neighboring cells or dendrites of

other neurons via a small gap called the synaptic cleft with a separation distance that varies from 20 to 40 nm.[2]

Neuronal communication often occurs at specified sites called synapses and this is thus called synaptic transmission. There are two types of synaptic transmission: chemical and electrical. Chemical synaptic transmission is the main process of cellular signaling. Normally, an electric impulse starts in the cell body, travels down the axon and invades the axon terminal. At the chemical synapse, the arrival of the electric impulse induces the release of chemical transmitters which then diffuse across the synaptic cleft and bind to specific receptors on the plasma membrane of the receiving neurons. Once they bind to the receptors, these chemical signals are converted into electrical impulses that are transmitted toward the soma of the receiving neuron. This process can go on along a network containing many neurons. In addition to transmitters being released in the synapse, the release of transmitters has been shown to take place at extrasynaptic sites including the cell soma and the dendrites.[3] A second type of synaptic transmission, called electrical transmission, is also found in the central nervous system. In this form of communication, the membranes of two neurons are really close together (about 4 nm) and physically linked by intercellular channels to form gap junctions. Unlike chemical synaptic transmission using chemical transmitters for signal transduction, electrical synaptic transmission utilizes ion currents that flow directly across the gap junction pores from one neuron to another. Thus, signaling in electrical synapses is instantaneous and less likely to be blocked. The main role of electrical synapse is to synchronize the electrical activity of a number of neurons.

1.2   Signal transmission within nerve cells

Signal transmission occurring along a nerve cell depends on differences in the membrane potential between inside and outside of the cell. A variety of ions, such as Na^+, K^+, Cl^-, and Ca^{2+}, are distributed unevenly across the membrane and this generates a Nernstian or membrane potential. All these ions can cross the cellular membrane via ion channels with varying permeability, and Na^+, K^+ are actively pumped across via the Na/K pump. At the resting state when no signal is transmitted, the membrane potential measured inside to outside is approximately in the range of -80 to -40 mV. When an action potential arrives at an axon terminal, it causes the depolarization of the membrane which opens voltage-sensitive Ca^{2+} channels in the nerve terminal. The influx of Ca^{2+} ions triggers the SNARE complex (this is a group of proteins) to initiate the vesicle fusion at the

plasma membrane. As a result, chemical transmitters are released through fusion pores formed between the vesicle and the cell membrane. These than travel across the synaptic cleft to bind to receptors embedded in the plasma membrane of nearby neurons. The binding of the transmitters induces a change in permeability for ions across the membrane, which, if excitatory, produces an action potential in the receiving cell. For cellular signaling to function properly, the extracellular transmitter levels need to be brought back to normal. After binding, the released transmitters are inactivated by reuptake or breakdown which is performed by transporters and enzymes on the membrane.

Synaptic transmission can be fast, taking place within several milliseconds, whereas slow synaptic transmission occurs in seconds or minutes. These transmissions depend on the type of the receptors activated by the released transmitters. These receptors are classified as ligand-gated ion channels or G-protein coupled receptors. Ligand-gated ion channels are responsible for fast synaptic transmission.[4] When a transmitter activates a ligand-gated ion channel, this receptor undergoes a conformational change leading to the opening of the gate and causing the diffusion of ions across the membrane. Slow synaptic signaling occurs as G-protein coupled receptors are activated. In response to the binding of transmitters, associated G proteins are stimulated resulting in the generation of second messenger molecules that directly modulate ion channels.[5]
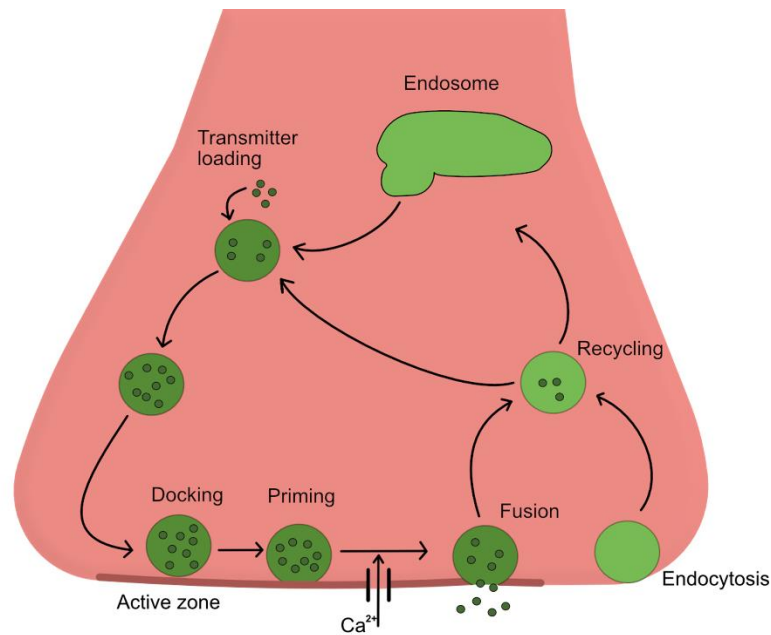

Figure 1.2. Exocytotic process takes place at the synapse of a neuron. Transmitters are loaded into synaptic vesicles. In preparation for exocytosis, vesicles are transported into the plasma membrane for docking and priming. Exocytosis is then triggered by the increase of

cytosolic Ca^{2+} and transmitters are released into the synaptic cleft. After release, vesicles are recycled via different pathways.

Most cell-to-cell signaling depends on the process termed exocytosis that regulates the release of chemical transmitters. Figure 1.2 illustrates many steps involved in exocytosis cycle including docking, priming, and fusion. Numerous transmitters are synthesized at the axon terminal and packed in synaptic vesicles. In preparation for synaptic exocytosis, these vesicles are transported to the site of release and then docked at the plasma membrane of the active zone. Since docking always takes place at the active zone, it has been suggested that there is a recognition reaction between the synaptic vesicle and the protein at the active zone. After docking, the vesicles are primed by an ATP-dependent process.[6] Once the plasma membrane is depolarized, an increase in intracellular Ca^{2+} leads to the fusion reaction. This occurs as something called the SNARE complex undergoes a conformational change induced by interacting with Ca^{2+} ions. These proteins create a linkage between the vesicle and the cell membrane bringing them close enough to fuse.[7] The secretion of vesicle contents can occur through different modes of exocytosis. Until the last decades, the *full fusion* process has been believed to be the only exocytosis mode. In this mode, the vesicle membrane collapses after fusion and combines completely with the plasma membrane of the cell, thus all of vesicle contents are released.[8] Electrochemical techniques have been used to demonstrated other modes of exocytosis, one of which is called *kiss-and-run*. Here, a small amount of transmitter is secreted through a narrow fusion pore. Recently, numerous studies using amperometry techniques have strongly suggested that most "*full*" exocytosis occurs through a *partial release* mode.[9-11] During the *kiss-and-run* and *partial release* processes, the fusion pore is closed after the releasing phase, thus the vesicular matrix remains inside. In contrast, after the *full fusion* exocytosis, the vesicle is totally merged with the plasma membrane and later recycled via the endocytosis process.

1.3 Impact of psychostimulants on neurotransmission

Psychostimulants, such as cocaine, methylphenidate, amphetamine, and methamphetamine, are sympathomimetic drugs, which produce euphoria and increase motor activity. Although psychostimulants have been used for various medical purposes, they have a high abuse potential leading to addiction. The precise mechanisms of psychostimulant action on the brain are not yet fully

understood. Current hypotheses suggest that psychostimulants produce their effects by promoting the neurotransmission in the brain, especially in the limbic regions.[12] Psychostimulants interact with several monoamine transporters including dopamine, norepinephrine, epinephrine, and serotonin transporters. The dopamine transporters, however, are primary targets for multiple psychostimulants that influence synaptic dopamine and many other biological processes. Cocaine and methylphenidate competitively bind to dopamine transporters and thus block dopamine reuptake (Figure 1.3). As a result, the dopamine molecules build up in the synaptic cleft and over-activate the receiving cells. Although the actions of amphetamine and methamphetamine are different compared to cocaine, they also require the interaction with dopamine transporters for their actions. Amphetamine and methamphetamine behave as competitive substrates for dopamine transporters and inhibit dopamine reuptake. They also penetrate into storage vesicles and act as weak bases to interrupt the pH gradient, which results in the release of dopamine from vesicle to cytoplasm.[13] The accumulated dopamine in the cytosol activates the dopamine transporter-mediated reverse transport of dopamine, thereby causing the release of dopamine into the extracellular space.

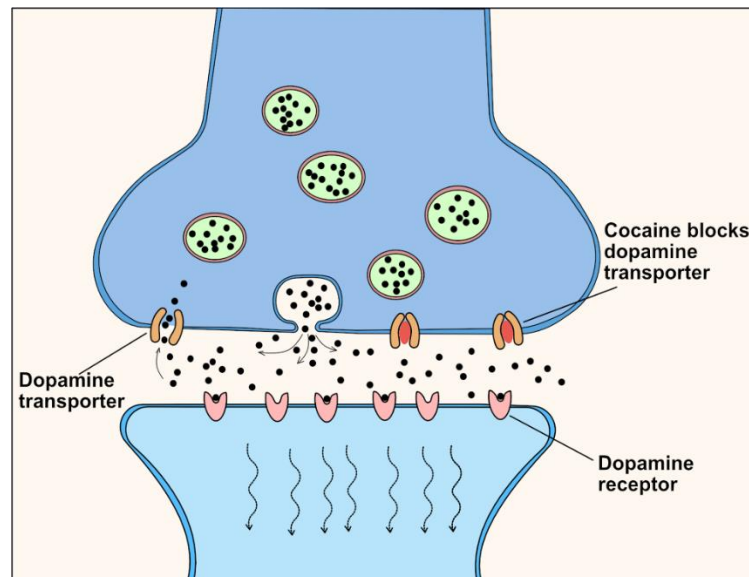Figure 1.3. Cocaine induces the elevation of extracellular dopamine levels by blocking dopamine reuptake.

The use of psychostimulants is thought to induce the disruption or modification of normal neurotransmission by significant dysregulation of the dopamine system. Chronic cocaine and methamphetamine lead to the persistent depletion of dopamine levels in the brain.[14] This dopamine deficiency is thought to be

related to drug-seeking behaviors and a risk factor for common brain disorders, such as Alzheimer's disease and Parkinson disease.[15, 16] Psychostimulants, such as methylphenidate and modafinil, are prescribed at low doses to improve focus and cognition for treatment of attention deficit hyperactivity disorder, as well as to treat excessive sleepiness caused by narcolepsy. A growing body of literature, nevertheless, has demonstrated their abilities of psychostimulants, such as cocaine and amphetamine, to cause addiction and cognitive impairments including the disruption of learning/memory and attention, as well as poor decision making.[17] It is necessary to study the effects of drugs of abuse on cellular communication to get a better understanding of how these drugs induce changes in cognitive processes. Specially, the alterations in lipid metabolisms induced by psychostimulants has been suggested as a key factor associated with cognitive deficit and will be discussed further in the next chapter. Targeting on cognitive enhancement, thus, may open new possible therapies to improve treatment outcomes for addiction.

1.4 Classical neuroscience approaches to measure the impact of drugs on synaptic transmission

Synaptic transmission is a key player in normal functioning of the brain that ranges from regulation of movement and mood to cognition, learning and memory, as well as decision making. In recent decades, new approaches have been developed to elucidate how synapses work molecularly. One of the classical electrophysiological techniques used is called patch clamp. This measures the alterations in membrane capacitance after vesicle fusion.[18, 19] In this method, a glass pipette is placed onto a small area of membrane surface to make a tight contact with the membrane. Several modes of patch clamp have been invented and its discovery was awarded the 1991 Nobel Prize. In the cell-attached patch mode, gentle suction is applied to draw a part of the membrane into the tip, which creates a resistive seal. In the whole cell patch clamp mode, a strong pulse of suction is used to break through the membrane completely. As a result, the cytoplasm of the cell is continuous with the solution in the pipette. This set-up can be used to measure the potential, current, or capacitance from the entire cell. Another technique, called amperometry, using a small carbon fiber electrode to study cellular exocytosis in a single cell was originally developed by Wightman and colleagues.[20, 21] Here, the electrode is placed on the surface of a single cell

during stimulation of transmitter release. Each release of transmitters from a single vesicle is recorded as a current trace known as a spike. The shape of the spike provides information about vesicle fusion including fusion pore formation, expansion of the pore, the release of transmitters into the extracellular space, and finally the pore closure. In addition, the amount of transmitters released can be quantified by the area of the spike. Amperometry is the only method to date that can be used to count the number of molecules released during exocytosis. This approach has been improved and applied for various cell types. In the last few decades, Lindau and colleagues developed another new technique which combined patch-clamp electrophysiology and amperometry.[22] Here, the carbon fiber electrode is placed inside a patch pipette to obtain the size of a single vesicle as well as the amount and kinetics of transmitter released from the same vesicle and this is called patch amperometry.

While electrophysiological and electrochemical techniques provide the quantification of transmitters release, their spatial resolution is still limited. Imaging techniques, involving fluorescent staining of vesicles, have been introduced to visualize and measure the exocytotic process in real time.[23] The use of several fluorescent probes to label vesicle membranes and vesicle content has been developed. One of the styryl dyes, FM1-43, is widely used to label inside vesicle membranes during cell stimulation to undergo exocytosis. The uptake of FM1-43 into recycle vesicles makes it possible to study vesicle exocytosis and recycling.[24] For instance, Stevens *et al.* identified the special state of exocytosis with *"kiss-and-run"* at hippocampus synapses.[25] Recently, new optical probes, FFN511 and the pH sensitive analog Mini202, have been synthesized to image the dynamics of release during exocytosis.[26, 27] Briefly, these molecules are false transmitters and can be loaded into vesicles to monitor release. In one example of stimulation of PC12 cells loaded with FFN, these vesicles were triggered to release their contents including the dyes and thereby the depletion of fluorescence obtained.[28] The work provides a new opportunity to image and quantitatively measure the kinetics of the released transmitters during exocytosis.

Chapter 2

Membrane lipids and important roles of lipids in cellular processes

The general term "lipid" is used to refer to a group of organic molecules which poorly dissolve in water, but readily dissolve in non-polar solvents. Various studies of lipids have recognized the important roles of lipid molecules in a variety of biochemical functions, such as acting as key components of the cellular membrane, involvement in energy storage and in signal transduction. Due to their importance, disturbances of lipid structures, composition, or metabolism are associated with impairment in brain function as well as a number of diseases, for example neurodegenerative diseases, cancers, obesity, as well as diabetes.[29-32] There are several reasons that changes in lipid composition and metabolism might be changed in the body, and these include disease, diet, and drugs. In this chapter, I will introduce knowledge and key roles of lipid functions as well as discuss how drugs affect the pathways of lipid metabolism.

2.1 Diversity in lipid structures

Lipids have a great diversity in their structures with approximate 2000 species. Therefore, it is essential to develop the comprehensive classification system for lipids. In general, lipids are usually subdivided into simple and complex lipids which is convenient for analytical purposes. Simple lipids, such as fatty acids, acylglycerols, and sterols, refer to *neutral lipids* which yield at most two products upon hydrolysis. In contrast, complex lipids or *polar lipids*, i.e. glycerophospholipids and sphingolipids, yield three or more products on hydrolysis per mole. However, the terms *neutral* and *polar lipids* are not precise and may cause confusion in the determination of their groups. Recently, the LIPID MAPS Lipid Classification System has provided more accurate definitions to classify lipid molecules based on their structural and biosynthetic perspectives. This system is comprised of 8 primary classes: fatty acids, glycerolipids, glycerophospholipids, sphingolipids, saccharolipids, polyketides, sterol lipids,

and prenol lipids.[33] In the next sections, structures and synthesis of the most common lipid categories found in biological system are discussed.

2.1.1 Fatty acids

Fatty acids (FAs) have diverse functions in cells that range from building blocks of complex lipids to acting as energy storage sources and signaling molecules. The FAs are usually characterized by hydrocarbon chains linked to a terminal carboxylic acid (-COOH) (Figure 2.1). The main FAs in plants and animals consist of even numbers of carbon atoms in straight chains classified as either saturated or unsaturated. The saturated FAs contain a carbon chain saturated with hydrogen atoms. Saturated FAs, that have a straight-chain from 14 to 22 carbon atoms in the chain length, represent the most abundant subclass of FAs in animal and plant tissues. Variants of this subclass are the branched-chain FAs bearing one or more methyl substituents along the chain length. The branched chain FAs are more complex molecules and are rarely found in natural biological systems. Additionally, FAs can contain one or multiple double bonds in the *cis* configuration and are then called monounsaturated FAs (MUFAs) or polyunsaturated FAs (PUFAs), respectively. One of the most abundant MUFAs is oleic acid with short nomenclature as FA (18:1) where "18" is the number of carbon atoms in the chain and "1" is the total number of double bonds. Likewise, linoleic acid, FA (18:2), and linolenic acid, FA (18:3), are commonly found in the PUFA subclass. Linoleic acid (omega-6) and linolenic acid (omega-3) are essential in development and metabolism, the immune response, and to provide anti-oxidative properties. However, they cannot be synthesized in the human body and are obtained via the diet. Except these two PUFAs, our body can synthesize most of FAs by sequences of reactions catalyzed by different enzymes.[34] FA synthesis starts from the formation of malonyl Coenzyme A (CoA) by carboxylation of acetyl CoA. Malonyl CoA and acetyl CoA are attached to different protein carriers to create malonyl ACP and acetyl ACP. The newly formed malonyl ACP and acetyl ACP are then combined to generate the 4-carbon molecule acetoacetyl-ACP and CO_2. The CO group in acetoacetyl-ACP is converted into a hydrocarbon group leading to the generation of hydrocarbon FA linked to ACP. This process is repeated many times and thus generates FA at the end of the chain of reactions. The double bonds can be introduced into specific positions of the long-chain FAs by a desaturation process. There are different desaturase enzymes which decide the positions and numbers of double bonds added to the carbon chains. The most common desaturase enzymes present in

humans are the Δ9, Δ5, and Δ6 desaturases.[35] Δ9 desaturase is required for synthesis of MUFAs, whereas Δ5, and Δ6 desaturase are used to synthesize PUFAs.

Saturated fatty acid

Stearic acid, FA (18:0)

Unsaturated fatty acid
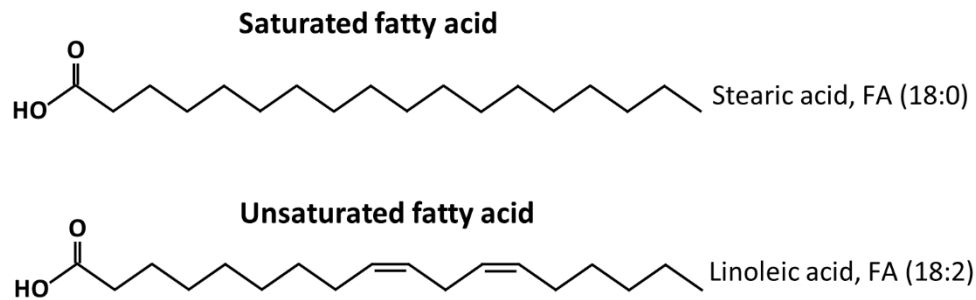
Linoleic acid, FA (18:2)

Figure 2.1. General structure of saturated and unsaturated FAs.

2.1.2 Glycerolipids

The basic structure of glycerolipids is a glycerol backbone, which forms a link to FA chains by an ester or ether bond. Glycerolipids consist of mono-, di-, and tri-substituted glycerol (Figure 2.2).

Triacylglycerol   **Diacylglycerol**   **Monoacylglycerol**
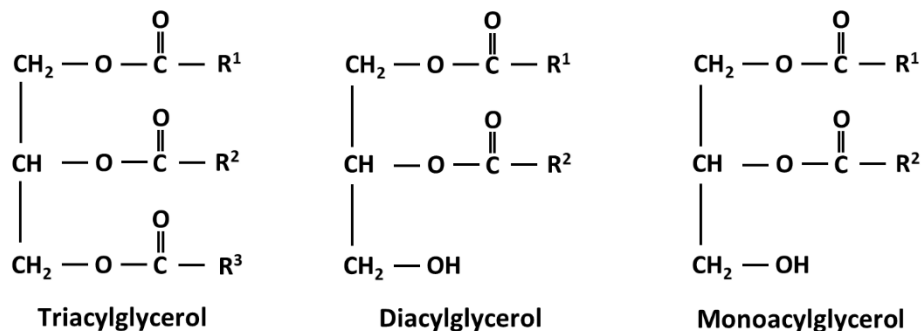
Figure 2.2. Structure of glycerolipids includes mono-, di-, and tri-substituted glycerol. R is the hydrocarbon chain of FA.

Triacylglycerols

Triacylglycerol (TAG) is the best known glycerolipid and consists of three FAs esterified to glycerol. The TAG molecule mainly serves as storage source providing precursors (FAs and diacylglycerols) for membrane lipid synthesis. The synthesis of TAG is carried out primarily in the adipose tissue and liver via the glycerol-3-phosphate or the monoacylglycerol pathway, and takes place in both the endoplasmic reticulum (ER) and the mitochondria. After synthesis, TAGs are packed in the core of cytoplasmic lipid droplets which are wrapped in a monolayer of glycerophospholipids in the adipose tissue.[36] These lipid droplets regulate the hydrolysis process of TAG degradation, also known as lipolysis, to

balance the energy storage and utilization. During lipolysis, TAG is converted into diacylglycerol and FA. Diacylglycerol is then further broken down to monoacylglycerol.

Diacylglycerol

Diacylglycerols (DAGs), which contain two FAs, are only found in small amounts in animal tissues. DAGs serve as components of cellular membranes as well as being involved in several metabolic pathways. DAGs accumulate transiently in the membrane via strong hydrophobic interactions with proteins and then modify the physical properties of the cell membrane. When DAGs concentrate in small areas of membrane, they induce unstable negative curvature because they lack charge and have a smaller head group compared to carbon chain size. This negative curvature is essential for membrane fusion and fission processes. Another role of DAGs is that they act as a lipid second messengers to activate protein kinase C.[37] DAGs are generated by two main pathways in yeast and mammals with two different precursors: glycerol-3-phosphate and dihydroxyacetone-3-phosphate. In addition to main pathways, there are three alternative pathways that produce DAGs via many reactions catalyzed by sphingomyelin synthase, phospholipase C, and phospholipase D.[38]

Monoacylglycerol

Monoacylglycerols (MAGs) contain a FA attached in a glycerol backbone via an ester linkage in the form of 1-monoacylglycerol or isomeric 2-monoacylglycerol. They are found naturally at low levels in plants and animals. As mentioned above, MAGs are generated by hydrolysis of DAGs by DAG lipase.
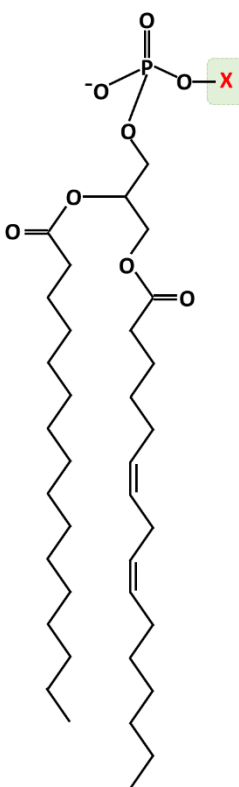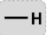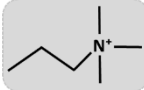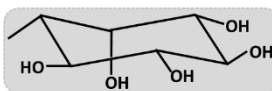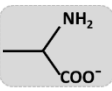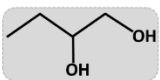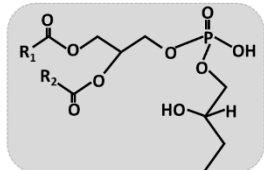
2.1.3 Glycerophospholipids

Glycerophospholipids, also known as phospholipids, are the major components in eukaryotic membranes. They are composed of two non-polar FA tails, a glycerol backbone, and a phosphate group with a head group substituent (Table 2.1). The glycerophospholipids can be categorized into several subclasses based on their structures of head group at the sn-3 position of the glycerol backbone, with choline, ethanolamine, serine, inositol, as well as other less frequent groups. In addition, the length and saturation of hydrophobic FA chains determine the different physical properties and functions of glycerophospholipids. Synthesis of

glycerophospholipids mainly occurs in the ER of the cell and its specific domain, mitochondria-associated membrane, using two common precursors: phosphatidic acid and DAG (Figure 2.3).[39, 40]

Table 2.1. General structure of a glycerophospholipid consists of two hydrophobic FA chains and a phosphate group with a different head group substituent, x.

Basic glycerophospholipid structure	Substituents X	Glycerophospholipids	Net charge (at pH 7)
	Hydrogen	Phosphatidic acid	-1 anionic
	Choline	Phosphatidylcholine	0 zwitterionic
	Ethanolamine	Phosphatidylethanolamine	0 zwitterionic
	Inositol	Phosphatidylinositol	-1 anionic
	Serine	Phosphatidylserine	-1 anionic
	Glycerol	Phosphatidylglycerol	-1 anionic
	Phosphatidylglycerol	Cardiolipin	-2 anionic
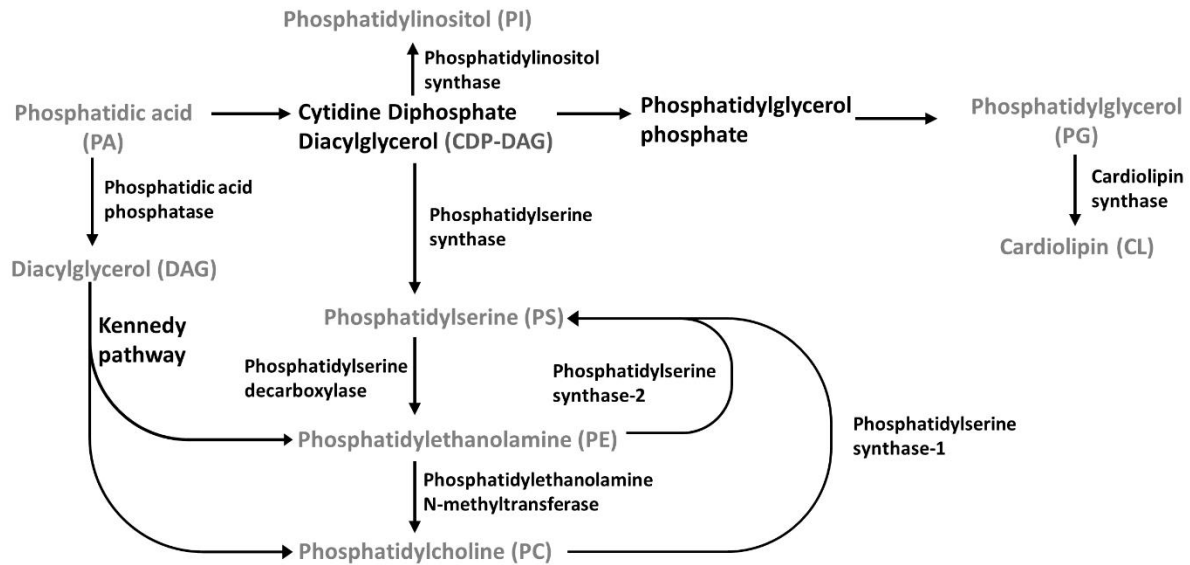
Figure 2.3. Glycerophospholipids are generated from phosphatidic acid through a variety of synthetic pathways.

Phosphatidic acid

Phosphatidic acid (PA) is the smallest and simplest glycerophospholipid and consists of two acyl chains and a hydrogen atom as a head group. Although appearing at low levels in total membrane lipids, PA is the original precursor for most of membrane glycerophospholipids. PA with small head group contributes to membrane curvature even though PA comprises a very small fraction of lipid membrane. Beside its role as a precursor for other glycerophospholipids, PA also plays various roles in cellular signaling and cellular functions, such as cell proliferation, vesicle/membrane trafficking, and cytoskeletal organization.[41] PA can carry one or two negative charges in the phosphate group, which can attract positively charged molecules. For example, Ca^{2+} bound to membrane PAs creates the domain which is sensitive to pH, temperature, and cation concentration.

In mammals, PA is synthesized via different enzymatic pathways.[42] Structural PAs are usually synthesized via the glycerol-3-phosphate pathway and dihydroxyacetone phosphate. Moreover, PAs are generated by hydrolysis of phosphatidylcholine by phospholipase D. Another pathway is the acylation of lysoPA.

Phosphatidylcholine

The head group substituent of phosphatidylcholines (PCs) is choline, which contains a positive charge. The positively charged head group together with a negatively charged phosphate group make PC a zwitterionic molecule. PC is the

most abundant glycerophospholipid in eukaryotic cells, comprising about 40-50% of total glycerophospholipids. It is found to be abundant in the outer leaflet of the membranes. PC is not only a major component of the cellular membrane, but also a major source of many signaling molecules such as DAG, PA, choline, lysoPA, and lysoPC. PC molecules are synthesized primarily through the CDP/Kennedy pathway.[43] First, choline is rapidly phosphorylated and then coupled to cytidine diphosphocholine (CDP) to generate CDP-choline. An enzyme, choline phosphotransferase transfers CDP-choline to DAG and consequently the production of PC. An alternative pathway for PC synthesis is the phosphatidylethanolamine N-methyltransferase pathway where phosphatidylethanolamine is converted to PC by sequential methylation reactions.[44]

Phosphatidylethanolamine

The second most abundant glycerophospholipid in eukaryotic cells is phosphatidylethanolamine (PE), which composes 25% of all glycerophospholipids. PE is asymmetrically distributed across the bilayer membrane, but it is normally enriched on the inner leaflet of membranes. Beyond serving as a membrane component, PE is also a key player in a variety of cellular functions that range from serving as a precursor for other lipids and promoting membrane deformation during fusion and fission events.[45] PE is zwitterionic with a phosphate group (negative charge) and ethanolamine head group (positive charge). The positively charged head group of PE can strongly bind to a neighboring glycerophospholipid or membrane proteins. Similar to PC, the biosynthesis of PE in mammalian cells takes place mainly in the ER via the Kennedy pathway in which the CDP-ethanolamine is attached to DAG by the enzyme ethanolamine phosphotransferase.[43] The second major pathway for PE synthesis is the phosphatidylserine decarboxylation pathway, as originally described by Borkenhagen *et al.* in 1961.[46] This reaction takes place in the inner membrane of mitochondria where an enzyme decarboxylates phosphatidylserine to PE. In addition, small amounts of PE can also be generated in mammalian cells from a base-exchange reaction catalyzed by phosphatidylserine synthase-2 in the ER.[47]

Phosphatidylinositol

Although making up only a small fraction of cellular glycerophospholipids, phosphatidylinositol (PI) regulates many key biological processes. PI regulates

ion channels, pumps, and transporters, and also controls exocytosis and endocytosis. PI biosynthesis in eukaryotic cells occurs in the ER and uses a PI synthase enzyme as a catalyst for the reaction of CDP-DAG and myo-inositol to generate PI.[48] The newly formed PI is then transferred throughout the cell by several PI transfer proteins or possibly via vesicular trafficking. The inositol ring of the PI head group can be phosphorylated at three different positions 3, 4, 5, thus resulting in seven possible forms of phosphoinositides (PIPs). Among these PIPs, phosphatidylinositol 4-phosphate PI(4)P and phosphatidylinositol 4,5-biphosphate (PI(4,5)P_2) are the most abundant in the cell membrane. PI constitutes about 10-20% of total glycerophospholipids, whereas the abundance of PI(4)P and PI(4,5)P2 is about 1%.[49] The signaling functions of PIPs, such as lipid signaling and intracellular vesicle trafficking, have been desmonstrated.[50] Moreover, the inositol ring in the membrane acts as a binding site for cytosolic or membrane proteins which are involved in many cellular processes. For instance, PI(4,5)P_2-binding to proteins interacts with the SNARE protein complex to stimulate the assembly for membrane fusion during vesicle exocytosis.[51]

Phosphatidylserine

Phosphatidylserine (PS), which contains serine as a head group substituent, is present as a minor constituent of biological membranes, less than 10%. Although appearing in small amounts, PS contributes to various physical and biochemical properties. PS is a key player in the activation of enzymes, and cell cycle signaling, especially apoptosis.[52] Similar to other glycerophospholipids, PS is distributed unevenly in the plasma membrane of cells. Although PS is found preferably in the inner leaflet of the plasma membrane, it can redistribute to the outer leaflet during apoptosis or platelet activation. Its relocation is believed to serve as signal recognition for phagocytosis of apoptotic cells, or blood coagulation. In mammalian tissues, PC and PE are utilized as substrates for PS production. PS is synthesized from PC and PE by exchanging the head groups, choline or ethanolamine, with serine. This reaction is catalyzed by PS synthase-1 and PS synthase-2 which are enriched in a mitochondria-associated membrane.[45]

Phosphatidylglycerol

Phosphatidylglycerol (PG) is a major component in the bacterial membrane, while it presents at low amounts (1-2% of total glycerophospholipids) in animal tissues. Glycerol serves as the PG head group, which does not compensate for

negative charge in phosphate group. As a result, PG provides a negative charge to the membrane as well as to lipid-protein interactions. Furthermore, CDP-DAG is also used for synthesis of PG in mitochondria. PG phosphate, produced from CDP-DAG, is dephosphorylated to form PG.[53]

Cardiolipin

Cardiolipin (CL) is an anionic glycerophospholipid which is most abundant in the heart and found in most animal tissues. CL is localized exclusively in mitochondria with high concentrations in the inner leaflet of the mitochondrial membrane. Unlike other membrane lipids that are generated in the ER, the *de novo* biosynthesis of CL occurs in mitochondria by using PG as a precursor. CL is generated by the addition of a phosphatidyl group into a PG molecule from a CDP-DAG molecule.[53] CL has a dimeric structure consisting of two PA molecules connected by a glycerol (Figure 2.4). Owing to four FA chains and two phosphate groups, CL has hydrophobic and acidic properties providing both hydrophobic and electrostatic interactions with membrane proteins in mitochondria. The lipid-protein interactions allow CL to participate in many mitochondrial processes including electron transport, protein transport, ion permeability and energy conversion.[54, 55] Interestingly, CL is translocated from the inner to outer mitochondrial membrane to serve as a binding site for signaling molecules. As CL has important roles in mitochondrial processes, disruption of CL metabolism induces serious diseases and many problems in heath. Changes in the CL pool lead to mitochondrial failure, which is associated with cardiac diseases.[56] A deficiency in CL biogenesis is linked to Barth syndrome, which is characterized by dilated cardiomyopathy, skeletal myopathy, and growth retardation and neutropenia.[57]
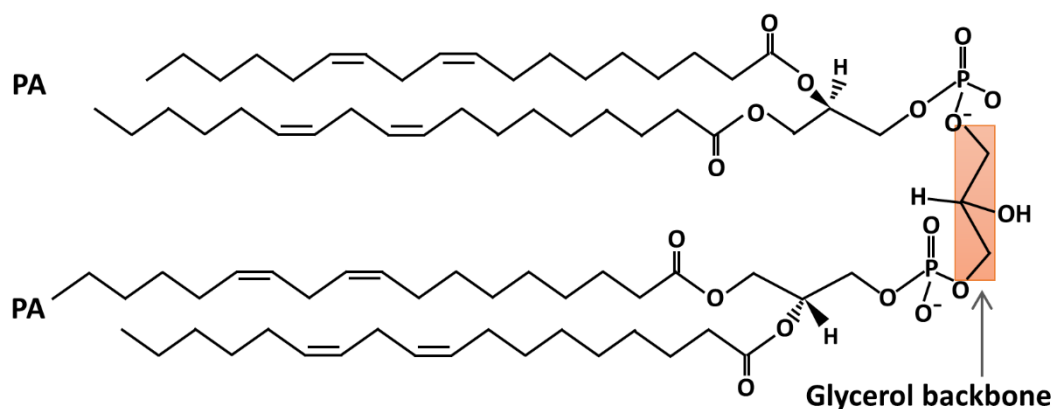
Figure 2.4. General structure of cardiolipin includes two PA molecules attached to a glycerol.

2.1.4 Sphingolipids

Sphingolipids are a major class of lipids in eukaryotic membranes, especially in brain and nerve tissue. Sphingolipids consists of a sphingosine backbone linked to FAs via an amide bond (Figure 2.5). The sphingosine backbone usually is a long-chain amino alcohol with 14-22 carbon atoms. It is believed that sphingolipids perform important functions in signaling processes involved in cell growth, differentiation, senescence, and apoptosis.[58]
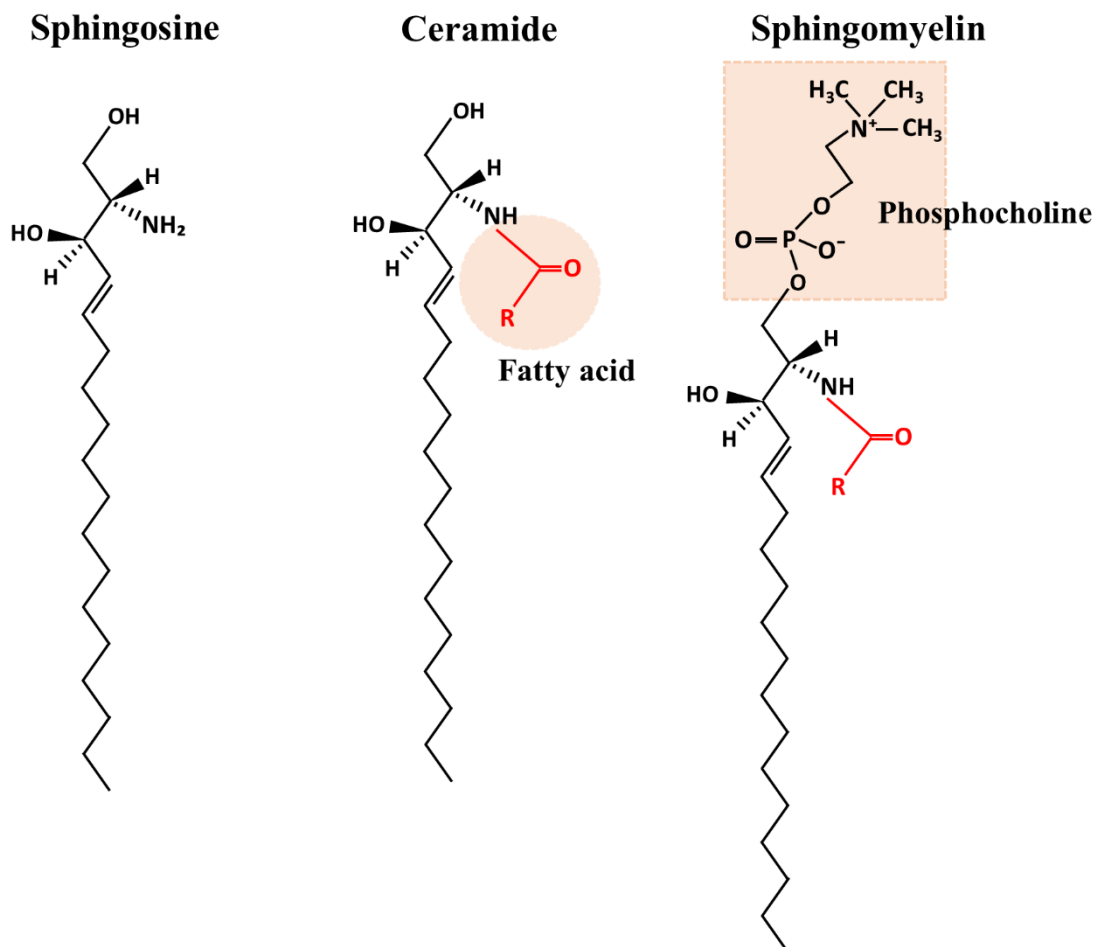
Figure 2.5. General structure of sphingolipids with sphingosine backbone, ceramide and sphingomyelin.

Ceramide

The simplest sphingolipid is ceramide, which is characterized by having a sphingosine base in an amide linkage with a FA. In mammals, ceramides are the building blocks of all sphingolipids as well as being a bioactive molecule that participates in regulating signal transduction in differentiation, proliferation, and apoptosis.[59, 60] The sphingomyelin pathway causes the breakdown of membrane

sphingomyelin to ceramide which acts a second messenger for regulating the apoptotic process. Ceramide is distributed in the membrane bilayer and has effects on the packing/rigidity of membrane glycerophospholipids. Moreover, ceramide tends to self-aggregate into membrane microdomains (rafts or caveolae) in association with sphingomyelin and cholesterol.[61, 62] In addition, there are numerous ceramides found in human skin which are essential components of the intercellular lipids. Nowadays, ceramide is used in human skin care products because it maintains the water permeability barrier function of the skin by linking the protein-rich corneocytes into a waterproof barrier.[63] The *de novo* synthesis of ceramide occurs in the ER which starts from condensation of serine and palmitol CoA followed by several acylation and reduction reactions to form ceramide. After formation, ceramide is transferred from the ER to the Golgi apparatus by either vesicular trafficking or transfer protein for synthesis of other sphingolipid metabolites. An alternative pathway to produce ceramide is through degradation of higher-order sphingolipids. Alternations in ceramide metabolism are thought to connect to a variety of diseases, for example cancer, cardiovascular, autoimmune and neurodegenerative diseases.

Sphingomyelin

Sphingomyelin (SM) is one of the most abundant sphingolipids in mammalian cells, particularly the myelin sheets of neurons. SM together with PC are major constituents of cellular membranes. They both have phosphocholine head groups in common and are found predominantly in the outer leaflet of the plasma membrane. Unlike PC with two FAs, SM has only one FA attached to a sphingosine base. In addition to the primary role of SM as a membrane component, it is involved in many cellular functions and processes including endocytosis, protein regulation, signal transduction. SM is synthesized primarily in the Golgi apparatus from two precursors, ceramide and PC.[64] The phosphocholine from PC is transferred to the primary hydroxyl of ceramide by SM synthase-1, and thus form SM and DAG. Small amounts of SM are also made via SM synthase-2 in the plasma membrane.

2.1.5 Sterols

Sterols are membrane lipids which consist of a four ring rigid sterol with an alcohol group and hydrocarbon side chain (Figure 2.6). Sterols have been proposed as key molecules to maintain membrane fluidity by regulating ordering/disordering of membranes.
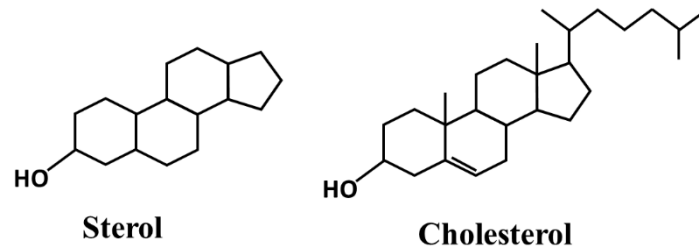
Figure 2.6. Structure of sterol and cholesterol.

Cholesterol

Cholesterol is the main sterol in animals, but not in plants, fungi, and bacteria. Cholesterol is a amphipathic molecule containing a polar group (hydroxyl group, –OH) and hydrophobic group (steroid ring and hydrocarbon) as seen in Figure 2.6. The hydroxyl group of cholesterol aligns toward the phosphate head groups of phospholipids while its hydrophobic region interacts with the FA tails of phospholipids. Cholesterol has different effects on membrane fluidity and permeability depending on temperature. At low temperature, the hydrogen bond between cholesterol and neighboring phospholipids is more stable and, hence, maintains membrane fluidity. In contrast, cholesterol has the opposite effect at high temperature. Cholesterol reduces the fluidity of membrane by interfering with the movement of the FA tails of phospholipids. Therefore, the permeability of membranes to small molecules is decreased. Recently, cholesterol has been suggested to associate with sphingolipids to form clusters called lipid rafts which perform an important role in signaling transduction.[65]

2.2 Lipid functions in biological system

2.2.1 Lipids as structural components of cell membranes

Lipids are the major structure components of cellular membranes which have a variety of key roles in biological functions in cells and tissues, especially the central nervous system. The primary function of lipids is to generate the bilayer barrier of cells and organelles (Figure 2.7).

Lipid molecules, which include a polar head group attached to non-polar FA chains, generate lipid bilayers around the cells. The interior of the lipid bilayer is filled by the hydrophobic FA chains and therefore the membrane is not permeable to water-soluble molecules including ions and biomolecules. Moreover, most of natural glycerophospholipids contain unsaturated hydrocarbon chains which make them difficult to pack together. Thus, the long hydrocarbon chains of the

FA tails can freely move in the interior of membrane and it is this ability that induces the flexibility of the membrane.
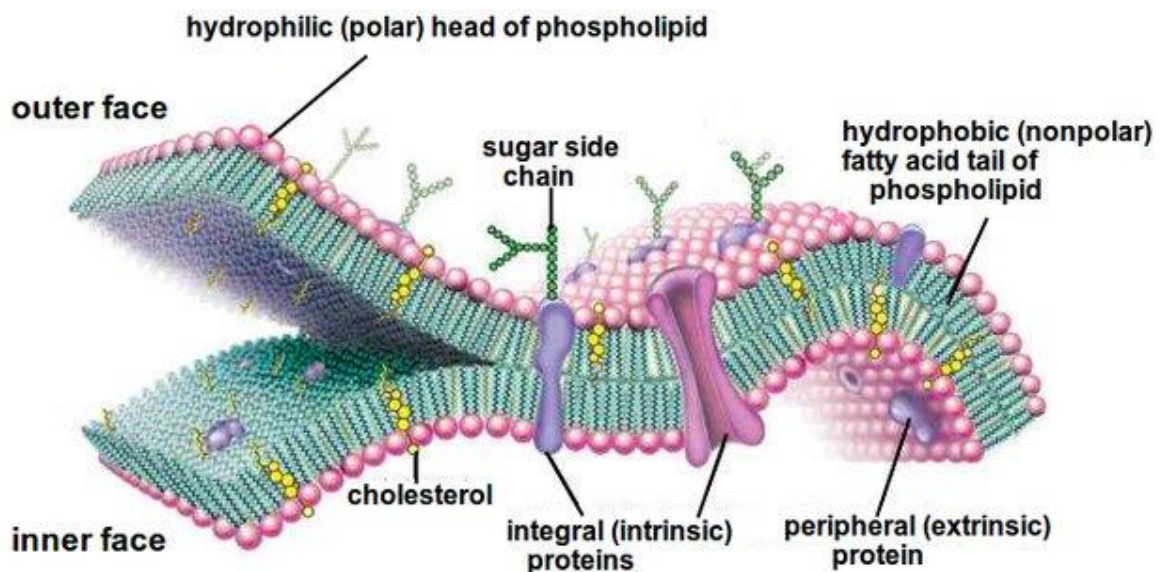
Figure 2.7. Model for structure of a cellular membrane. The model of eukaryotic plasma membrane was modified from Encyclopaedia Britanica, Inc. ©2020 https://www.britannica.com/science/membrane-biology.

Lipid bilayers are elastic, allowing them to resist the bending and stretching as well as to generate curvature for chemical trafficking. The geometric shape of individual lipids is determined by the space acquired for the area of the polar and non-polar groups (Figure 2.8). When the polar and non-polar groups require similar spaces, the lipid molecule is said to have a cylindrical shape. As a result, lamellar membrane structures are formed from these lipids. The cone shape lipids, which have a small head group and larger tails, induce the formation of negative curvature of the monolayer side of a bilayer. By contrast, inverted cone shape lipids, with large polar heads and small tails, cause positive curvature.
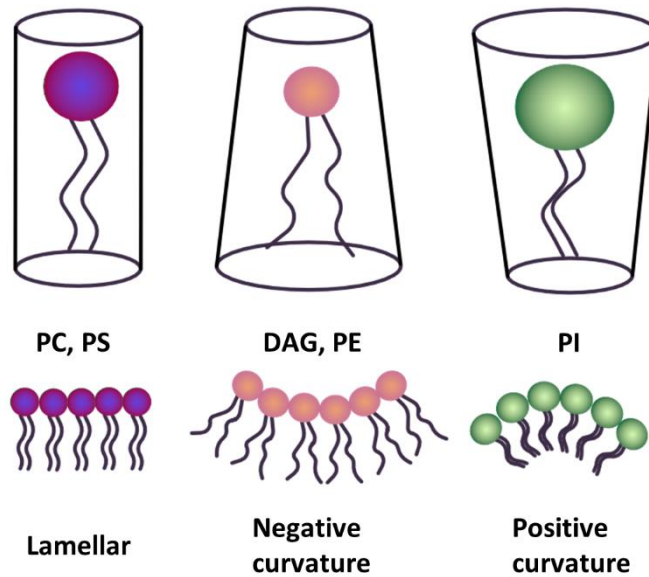
Figure 2.8. Lipids and membrane curvature. PC and PS give rise to a lamellar membrane. DAG and PE cause negative curvatures. PI generates a positive curvature.

2.2.2 Lipids acting as secondary messengers

In living organisms, cells communicate with each other and internally by use of chemical messengers. These chemical messengers are either water- or fat-soluble molecules. Fat-soluble chemical messengers can cross the membrane bilayer and cause a response by directly binding to internal receptors. However, water-soluble signaling molecules cannot pass through the membrane; therefore, their messages must be transduced across the membrane. The plasma membrane is not merely a barrier to separate and protect cellular internal organelles from the external environment. The membrane and its lipids also serve several key functions in signal transduction events. Signaling lipids regulate many important cellular processes including cell proliferation, apoptosis, and metabolism.

Although PI is a minor membrane component, it is a key element in cell signaling. Since the discovery of PI turn-over, $PI(4,5)P_2$, in 1980, the importance of this molecule in the signal transduction processes has been shown to be increasingly important. $PI(4,5)P_2$ is hydrolyzed by phospholipase C to generate second messenger molecules: membrane associated DAG and soluble inositol-1,4,5-trisphosphate. Inositol-1,4,5-trisphosphate stimulates the release of Ca^{2+} ions from the ER to promote cellular responses including transcription, cell growth and the immune response. Conversely, DAG activates protein kinase C, which then promotes the activity of a variety of kinases.[37] In parallel, $PI(4,5)P_2$ is converted to $PI(3,4,5)P_3$, which acts as a signaling lipid for regulation of cell growth, proliferation, and motility.[66] Interestingly, ceramides and sphingosines

also serve as signaling lipids in apoptosis.[67] Additionally, the converted product of sphingosine, sphingosine-1-phosphate, has a key role in promotion of cell growth and proliferation via the activation of different G protein-coupled receptors.[68]

2.3 Lipids versus proteins in regulation of transmission

The synaptic membrane and its lipids are knowledge to be key elements in vesicle release, also known as exocytosis. Exocytosis is an important process in the cell and is responsible for the release of signal molecules into the extracellular space to communicate with neighboring cells. Exocytosis is considered to be predominantly promoted by various proteins. It is also believed that lipids only perform a passive role, partially in membrane merging. However, recently an increasing number of studies have demonstrated that lipids have significant key functions in regulation of whole exocytosis process.[69] For instance, $PI(4,5)P_2$ molecules aggregate at the membrane fusion site and recruit numerous membrane proteins to the synaptic membrane.[70] These proteins, such as CAPS and Munc, bind to $PI(4,5)P_2$ to organize the SNARE proteins during vesicle priming. Growing studies support the important roles of phosphatidic acid, phosphatidylserine, and cholesterol in exocytosis.[71] In addition, lipids change the membrane topology for membrane fusion. During vesicle fusion, lipids form positive and negative curvatures in the membrane that are required to form a small opening pore to initiate release. Lipids with conical shapes including phosphatidylethanolamine, cholesterol, phosphatidic acid, or diacylglycerol promote the generation of negative curvatures. In contrast, inverted-conical lipids, such as phosphatidylserine, gangliosides, or lysophospholipids, form positive curvatures.[72]

2.4 Psychostimulant effects on remodeling of brain membrane lipids

The composition of membrane lipids can be altered associated with various conditions and diseases, such as medication, injuries, or neurodegenerative diseases. Among these conditions, psychostimulants have been shown to disturb different aspects of lipid metabolism that are accompanied by a variety of brain dysfunctions, especially cognitive performance, emotion, and motion. Psychostimulants, such as cocaine and methamphetamine, are highly abused

drugs that cause a dramatic elevation of extracellular levels of monoamines. Chronic administration of cocaine has been demonstrated to change the lipid compositions in the brain. Using electrospray ionization-mass spectrometry, Cumming *et al.* reported that repeated cocaine injections to male rats induced locomotor sensitization in parallel with the changes in the PC and PE levels in the hippocampus and the ventral striatum as well as the blood.[73] Additionally, opposite alterations of the distributions and relative abundance of lipids have been shown to occur by using mass spectrometry imaging following cocaine versus methylphenidate in *Drosophila melanogaster* brain.[74] Specially, methylphenidate induced the depletion of PC levels, whereas an elevation of PC concentration was observed after exposure to cocaine. Total PEs and PIs decreased with cocaine treatment, whereas these levels increased in fly brains treated with methylphenidate. This is explored in paper I and the lipid changes following cocaine removal in paper III. In addition to changes in phospholipids, cocaine causes elevation in gangliosides and neutral sphingolipids in rat offspring.[75] Similar to cocaine, chronic amphetamine induces the upregulation of quadrisialoganglioside and downregulation of monoganglioside 2, monoganglioside 3 and diganglioside 1 in the rat frontal cortex.[76] By application of mass spectrometry imaging, Bodzon-Kulakowska observed the elevation in the levels of PS, PG, and sulfatide species followed injection of morphine or cocaine in rat brain.[77] In contrast, amphetamine induced the depletion of PE and PS abundance.

The abuse of psychostimulants is a severe health problem worldwide. However, there is no effective medication for addiction by psychostimulants. The understanding of brain lipid metabolism associated with drug abuse provides a helpful value to develop the new therapy for drug addiction. Given the changes of lipids in the specific brain region, especially hippocampus, it is highly likely these lipid alterations are associated with aspects of drug addiction including drug-seeking urges and cognitive deficits. Thus, mechanisms to alter brain lipids should be a new target for pharmacological therapy in the near future to treat drug addiction and cognition impairment.

Chapter 3
Mass spectrometry imaging

Mass spectrometry imaging (MSI) has emerged as an important approach for simultaneously mapping multiple molecular species in a variety of samples. MSI is a label-free technique, which is capable of providing both chemical and spatial information for known and unknown molecules. One of the most applied MSI techniques is the sensitive surface technique of secondary ion mass spectrometry (SIMS). Owing to extensive fragmentation, the application of the SIMS technique is quite restricted in biological research. Currently, the development of the cluster ion sources opens up the potential of high-resolution imaging SIMS in the field of biotechnology. This chapter discusses briefly the history of MSI and the background of the SIMS technique. Finally, the application of time-of-flight SIMS (ToF-SIMS) in the analysis of biomaterials will be covered.

3.1   Short history of the field

Mass spectrometry (MS) has grown to be used as a tool in most scientific fields, particularly analytical chemistry. To appreciate how the MS field has had a rapid expansion till present date, it is necessary to look back at some inventors and the great advances in the field. The birth of MS has roots in nuclear physics and chemistry studies. At the end of 19th century, J. J. Thomson discovered "charges of negative electricity carried by particles of matter", later named electrons.[78] By using electric and magnetic fields to deflect cathode rays, also called electron beams, he could indirectly measure the mass of the electron. For his discovery of the electron, he was awarded the 1906 Nobel Prize in Physics.

Recognizing the great value of MS, Thomson's student, F. Aston, developed and built the first mass spectrometer to measure the masses of charged atoms by using parallel electric and magnetic fields.[79] Later on, Aston and his colleagues improved the instrument to separate and demonstrate the existence of elemental isotopes which won him the Nobel Prize in Chemistry in 1922.[80]

Until the 1940s, the technique of MS was still dominated by physics mainly to study the fundamental nature of atoms and particles. Later, A. Nier was successful in commercializing the instrument and showed the world the practicality of MS. He designed and built new mass analyzers, which were used in a variety of applications.[81, 82] He then developed a design named the Nier-Johnson mass

spectrometer, which was a combination of electrostatic and magnetic analyzers in a unique conformation. By the 1940s, MS was a useful technique established in several different fields.

In late 1940s, many new concepts in mass analyzers had evolved, several of which used time-varying electric fields to separate species with different masses instead of a magnetic field. In 1946, W. E. Stefens proposed the concept for the time-of-flight (ToF) mass spectrometer. In the ToF analyzer, ions with the same initial energy but different masses were separated when they flew down a long tube. Based on this principle, the first ToF mass spectrometer was built in 1948 by Cameron and Eggers.[83] In the early 1950s, W. Paul and H. Steinwedel initiated the development of the quadrupole mass analyzer and the quadrupole ion trap for mass analysis. In 1974, Fourier transform ion cyclotron resonance mass spectrometer was invented by M. B. Comisarow and A. G. Marshall providing the highest mass resolving power (m/Δm ~ 100.000) and mass accuracy (<1 ppm) still to date.[84]

SIMS was the first MS technique applied for chemical imaging. The novel concept of SIMS was published in 1949 by R. Herzog and F. Viehböck, in which two separated electric fields were used to accelerate primary and secondary ions.[85] The positive secondary ions emitted during the primary ion bombardment were accelerated and then analyzed in a Thomson parabola apparatus. SIMS was a hard ionization method, which was traditionally applied for elemental analysis. The earliest SIMS instrument was introduced in 1960s, which utilized an argon (Ar) primary beam with high current density to image elemental ions.[86] During the early time of SIMS, this technique was used for studying the surface of metals. In 1958, a static SIMS approach was proposed by A. Benninghoven producing an opportunity for surface analysis of organic molecules. This was obtained by using an ion beam with low current density which caused less damage of the desorbed molecules.[87]

By the 1980s, MS techniques were mainly applied for analysis of small organic molecules. Large biomolecules including proteins, peptides and nucleic acids, however, were a huge challenge. Almost at the same time, the developments of MS techniques including electrospray ionization (ESI) MS and matrix-assisted laser desorption/ionization (MALDI) MS were introduced. ESI and MALDI gave new possibilities in biology for the analysis of macromolecules. The inventors of ESI for MS analysis and for MALDI of proteins shared the 2002 Nobel Prize in chemistry for their development of these techniques. To this day, ESI and MALDI are still the methods of choice for studying proteins and peptides.

26

In parallel, several developments in primary ion sources of SIMS technique have been introduced that make SIMS techniques suitable for analysis of biological macromolecules.[88] Traditional SIMS instruments were equipped beams like Ar^+, gold (Au^+), cesium (Cs^+), oxygen (O^-), gallium (Ga^+), bismuth (Bi^+), and xenon (Xe^+) having high dose of an focused monoatomic primary ion to erode sample. The bombardment of the primary ion beam induced damage to the subsurface regions of the sample and produced small fragment species. This method was therefore suitable for elemental analysis. Hence, SIMS was frequently used for semi-conductors and metal analysis, but was limited for studying organic compounds. During the past decades, the rapid development of new cluster primary ion beams, particularly Au_n^+,[89] Bi_n^+,[90] sulfurpentafluoride (SF_5^+),[91] and C_{60}^+,[92] made the technique of SIMS capable of enhancing the ion yields for organic analysis.[93] With a primary ion beam comprised from several atoms, the subsurface damage is reduced, and the yields of higher mass fragments and intact molecules are significantly increased. Intriguingly, the gas cluster ion beam (GCIB) containing thousands of particles, like Ar_{500}^+ − Ar_{4000}^+ and $(CO_2)_{6000}^+$, minimizes the fragmentation due to low impact energy.[94, 95] GCIBs bring new chances for imaging intact molecules in complex biological samples with the technique of SIMS.

3.2 Mass spectrometry imaging

MSI is a popular tool in analytical fields which provides a chemical map of the sample surface. To generate a chemical image, a focused ion beam or laser is used to raster across the sample surface and acquires several spectra from different points on the sample surface. During the last decades, MSI has grown dramatically due to its broad applications that range from biomarker studies (lipids, proteins, peptides) to drug distributions.[96-98] Such wide applicability leads to the development of different techniques, particularly SIMS and MALDI. Since proposed in 1960s, the first imaging mass spectrometry, SIMS, has grown and developed quicky.[86, 99] During the early period of SIMS, this technique became valuable for studying inorganic materials.

Generally, among MSI approaches, SIMS offers the highest spatial resolution that ranges from micrometer to nanometer scale. SIMS is a relatively 'hard' ionization method compared to MALDI. A primary ion beam with high energy density is used to strike the sample material leading to the localized damage of sub-layers and breaking of intact molecules. SIMS, however, overcome these limitations with the invention of cluster ion beams (C_{60}^+, Ar_n^+). For instance, C_{60}^+

ion beams typically remove only a few monolayers and preserves the underlying layers while still increasing the yields of the intact molecules.[27]

The first MALDI imaging of biological tissues was described by Caprioli *et al.* in 1997.[100] Since then, MALDI has rapidly grown in its applications for the analysis of biological macromolecules. Although lacking in the area of low-mass information (≤1000 Da) and spatial resolution limitations, MALDI gives better detection of large molecular-weight species. MALDI imaging has been effective for characterization of large biomolecules including proteins, peptides, lipids, DNA and RNA – an application for which SIMS imaging has been restricted. Now, with the trend toward cluster ion sources in SIMS, it has been possible to target the mass range of 0 – 1000 Da, which makes it become a great complement to MALDI imaging.

3.3 Fundamentals of SIMS

SIMS has emerged as an important technique in biological research due to its high sensitivity, high mass resolution, high spatial resolution, as well as a wide range of masses at the low end. In SIMS, the sample surface is sputtered by energetic primary ions. The mechanism of this sputtering process can be characterized as a collision cascade of the particles.[101] As a primary ion carrying a few keV strikes the sample surface, its energy is transferred to atoms of the surface resulting in the collision cascade between atoms in the sample. Partial energy returns to the surface and gives the surface molecules sufficient energy to overcome surface binding energies; thus, causing the emission of secondary particles (Figure 3.1). Most of these sputtered particles are ejected as neutral atoms and molecules. A small fraction (about 1%) of these particles are ionized to positively and negatively charged ions called secondary ions. These secondary ions are collected and subsequently transferred into a mass analyzer, usually magnetic and electrostatic sectors or a ToF analyzer, where they are separated and analyzed based on their mass to charge ratios (*m/z*).
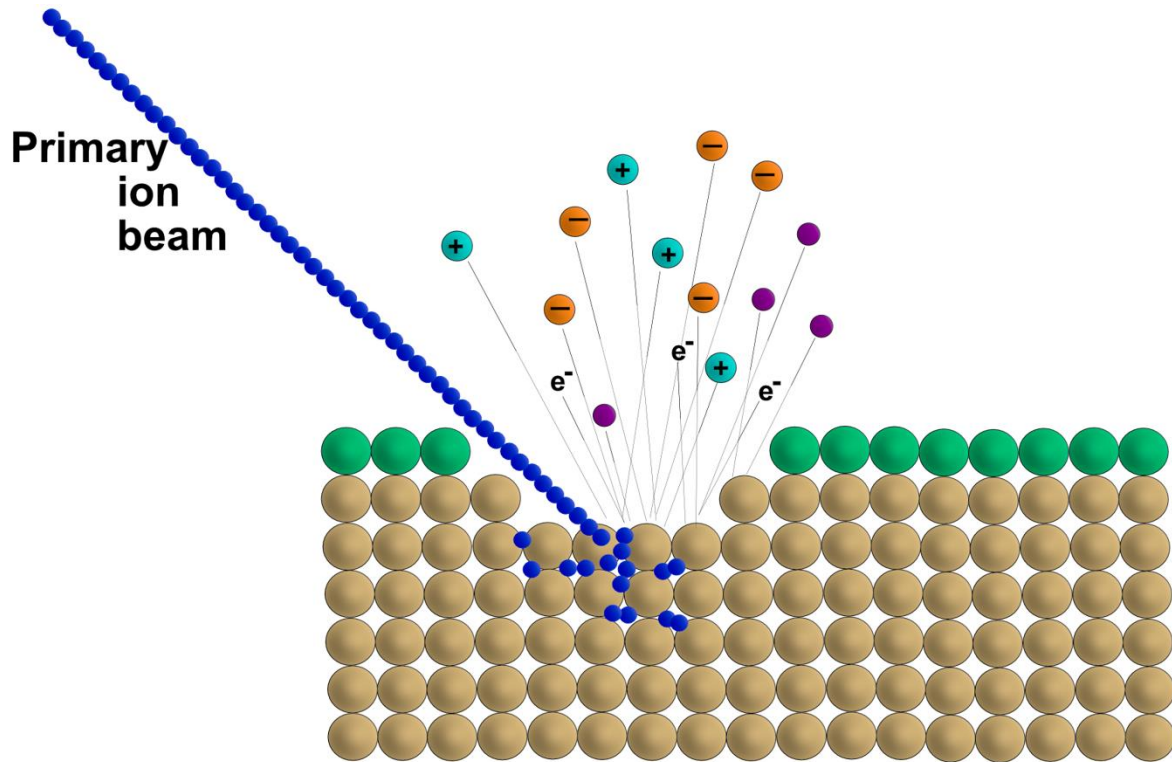
Figure 3.1. The schematic of the sputtering process in SIMS, where a focused primary ion beam is used to eject secondary particles along with electrons.

The formation of secondary ions, the ionization process, takes place close to the emission of sputtered particles and depends on the properties of the materials. The secondary ion intensity measured can be described by the SIMS equation, as shown below.

$$\mathbf{I_m = I_p Y_m \alpha \theta_m \eta} \tag{3.1}$$

Here, I_m is the secondary ion current of charged species m (counts/s)

I_p is the primary ion flux (ions/s)

Y_m is the sputter yield of species m per primary impact

α is the ionization probability of species m in positive or negative ion mode

θ_m is the fractional concentration of species m in the surface layer

η is the transmission of the analysis system

Based on the SIMS equation, the secondary ion intensity, I_m, is proportional to the concentration of the species. However, it is difficult to quantify the signal because of the matrix dependence of Y_m and α. This can be more complicated because of the matrix effect and surface charging. The matrix effect induces an alteration in the ionization rate of an analyte surrounded by other species. Surface analysis of materials with charged species leads to the buildup of

positive/negative charges on the surface called surface charging. This charging will attract the ions with opposite polarity causing the detected intensity of the analyzed ions to be reduced or even completely suppressed.

3.3.1 Sputter yield

The sputter yield is defined as the number of emitted atoms, including neutrals and ions, removed from the sample, per incident primary species. It elevates linearly with the primary ion flux. It also varies depending on the mass and energy of the primary particles, as well as the angle of incident primary beam, but not linearly. Primary particles with heavier mass lead to the energy depositing closer the surface and, thus, enhancing the sputter yield. The sputtering threshold energy of the primary particle for sputtering is at about 20-40 eV. The sputter yield shows a steep decrease at lower energies of the primary particles. This occurs because the atoms do not receive enough energy to overcome the surface binding energy. The sputter yield tends to reach maximum with the beam energy between 5-50 keV.[102, 103] Too high energy primary ions, over 50 keV, penetrate so deep into the sample and no energy returns to the surface. In addition, the sputter yield is also affected by the crystallinity and topography of the sample.

Sputtering is a damage process. The consequence of the sputtering process is the removal of elements, fragments, and molecular species from the sample. The loss of those species destroys the chemical structures within the sample area around the impact sites of the primary ions. This damage is characterized by a damage cross-section. With monoatomic primary ion beams, the damage is formed deeper into the materials due to the high energy per ion. For cluster ion beams, the ion energy is partitioned between all the atoms of the clusters. When cluster ions impact at a surface, the cluster breaks apart and each atom carries a low amount of energy causing the significant decrease in the penetration depth of the ions. This means that the chemical structure in the subsurface region is preserved. Atomic and molecular species are ejected much more gently from the surface than using the monoatomic ion beams. This phenomenon is defined as a non-linear cascade where parallel collisions occur simultaneously. Moreover, the cluster ion beams generate more atoms to bombard the sample surface, which produce the enhancements of the sputter yield. Cheng *et al.* demonstrated that the yield of several hundred molecules per impact was measured with a C_{60}^{+} primary ion beam sputtered the trehalose film.[104] Along with the C_{60}^{+} ion beam, benefits of using giant GCIBs (Ar_n for example) are currently obtained.[105] Cluster beams give many advantages for SIMS techniques that range from the enhancement of

high-mass ion yields to a reduction in charging and damage cross-section, as well as an ability to carry out molecular depth profiling.

3.3.2 Ionization probability

In order to improve the secondary ion yield, most advancements in SIMS have concentrated on total sputter yield, and only recently have they explored the enhancement of the ionization probability.[106-108] Owing to the static limit for nondestructive SIMS, much less than 1% of the ejected particles from the analyzed region are ionized. As a sputtered particle travels through the near-surface region, whether it escapes from the surface in an ionized state relies on its relative probability of ionization, α. The ionization probability α of a certain species can vary depending on the electronic properties and chemical nature of the sample. Thus, the secondary ion yield of that species is not directly proportional to the concentration of the species. This phenomenon is the so-called matrix effect. Hence, ToF-SIMS can be considered a semi-quantitative technique. For organic molecules, the secondary ion efficiency is usually low because of the poor ionization probability under the bombardment conditions.

The exact mechanisms of the secondary ion formation during the sputtering process in SIMS are still not completely understood. During the past few decades, various models for ionization processes have been suggested.[109-112] In principle, the ionization mechanisms in SIMS can be divided into physical and chemical ionization processes. The physical ionization mechanism involves an electron transfer processes. In the chemical ionization process, a chemical reaction occurs between an ejected neutral species M and some charged radical $R^{+,-}$. This reaction leads to the protonation/deprotonation events causing the formation of quasimolecular complexes like $[M+H]^+$, $[M+Na]^+$, $[M+Cl]^-$, or $[M+OH]^-$. For organic samples in SIMS, the most common quasimolecular ions are the protonated $[M+H]^+$ and deprotonated $[M-H]^-$ species. Other possible species include molecular radical $M^{+,-}$, loss of functional groups (e.g. $[M-CH_3]^+$), or alkali adduct ions (e.g. $[M+K]^+$).

As mentioned, the detection efficiency of organic molecules is still limited by the low level of the ionization probability. Improving α is crucially important to expand SIMS applications in the organic analysis. The addition of electronegative species, such as cesium or oxygen, leads to an enhancement in secondary-ionization probabilities. The neutral Cs atoms deposit on the specimen surface during the analysis. The presence of Cs enhances the negative secondary ion yields due to the electron transfer process. In contrast, oxygen is used to increase

the yield of positive secondary ions. The addition of oxygen leads to the oxidation of the sputtered atoms, especially metal atoms, around the ion impact region resulting in an increase in the ionization probability. Several researchers have realized that the presence of water in the frozen samples can increase the formation of $[M+H]^+$ ions owing to the formation of H_3O^+ in the sputtering area.[113] Moreover, doping small amounts of a chemically reactive species, such as CH_4, into the Ar GCIB results in the enhancement of protons in the impact zones compared to the bombardment of a pure Ar cluster ion beam.[30] Going further, the addition of salts or acids (for instance NaCl or HCl) elevates the formation of adduct ions $[M+X]^+$ or $[M+Y]^-$.[114, 115] The use of water cluster beams provides approximately 10 times higher in ion yields than Ar clusters.[116]

3.4 Different operation modes of SIMS: static versus dynamic SIMS

SIMS analysis traditionally has two operation modes: static and dynamic. Dynamic SIMS provides mainly elemental analysis and is usually preferred to determine the in-depth concentration of interested species. Conversely, static SIMS is often applied when one needs to identify both elemental and molecular information of surface species.

The first method is termed dynamic SIMS, which was the main mode of operation during the early days of SIMS. In dynamic SIMS, sample materials are eroded by the bombardment of a continuous primary ion beam with high energy ranging from 0.25 to 50 keV. The distribution of the kinetic energy of the primary ion near the surface has potentials to acquire spatial and depth information of chemical locations in samples. Although relatively large amounts of materials on the sample surface are rejected, the primary ions penetrate deep into the material resulting in the disruption of the sub-surface area of the sample. The direct impacts of the primary ions to atoms in the sample surface are highly energetic causing heavy fragmentation near the collision site. Hence, the atomic particles are produced, but molecular information is limited.

The dynamic SIMS approach usually uses monoatomic primary ion sources. The major advantage of these sources is the ability to focus the beam to considerably less than 1 µm, which gives great spatial resolution. Hence, dynamic SIMS is usually used in geological sciences and in semiconductor analysis. During the 1990s, a new ion beam configuration was described and became a useful dynamic SIMS performance at high lateral resolution.[117] This new

configuration was commercialized by CAMECA as the NanoSIMS 50 and 50L which combined great spatial resolution (approx. 50 nm), sensitivity (detecting 1 out of 20 nitrogen atoms and 1 out of 200 carbon atoms), and mass resolution (up to 10.000).[117, 118] Here, a highly focused primary ion beam was designed to be coaxial with the secondary beam extraction (Figure 3.2). The co-axial optics allow one shortening the working distance, enhancing the collection efficiency, as well as minimizing the shadowing effects. NanoSIMS is a destructive method, where the sample surface is continuously sputtered by an energetic primary ion beam, either Cs^+ or O^-, to produce the secondary ions. In a co-axial optical system, the secondary ions are collected back through the same lens assembly of the primary beam. The ions are sorted in an electrostatic sector based on their energies before entering to a mass analyzer where they are dispersed according to their energy. The NanoSIMS 50 and 50L contain 5-7 individual detectors, which are capable of imaging 5-7 elements or isotopes simultaneously. NanoSIMS imaging is applied mainly for the measurement of isotopic ratios and trace elements within geochemistry and material science. Recently, an interest in the NanoSIMS approach for the analysis of biomaterials and biological samples has grown rapidly. The high spatial resolution together with high mass resolution and high sensitivity make this technique capable of imaging stable isotope-labeled molecules at the single cell level.[119-121] For instance, the metabolic activity of single cells can be revealed with NanoSIMS by probing isotope distributions or elemental compositions. In addition, NanoSIMS imaging has had significant impact for tracer studies in single cells, such as cellular uptake and distribution of ^{15}N-labeled peptide vectors,[122] the transportation of fatty acid across the cell membrane,[123] and lipid distributions.[120, 124]

The formation of a collision cascade causes the destruction of molecules at the surface as well as in deeper layers. In order to minimize sample damage and promote the desorption of large fragments, a low primary ion dose has to be applied to sputter the materials at a few nanometers from the top layer of the sample surface. This approach is called static SIMS, described at the end of the 1960s.[103, 125] The use of a low primary ion density results in fewer primary ions striking the surface, and thus inducing less damage and less fragmentation. As discussed above, recent advances in cluster ion sources, bring opportunities to study from a wide range of biological samples. Owing to 'soft ionization', preservation of chemical bonds and molecular information in the fragments is possible. The cluster ion sources bring great promise for sub-micron spatial resolution for molecular SIMS imaging.
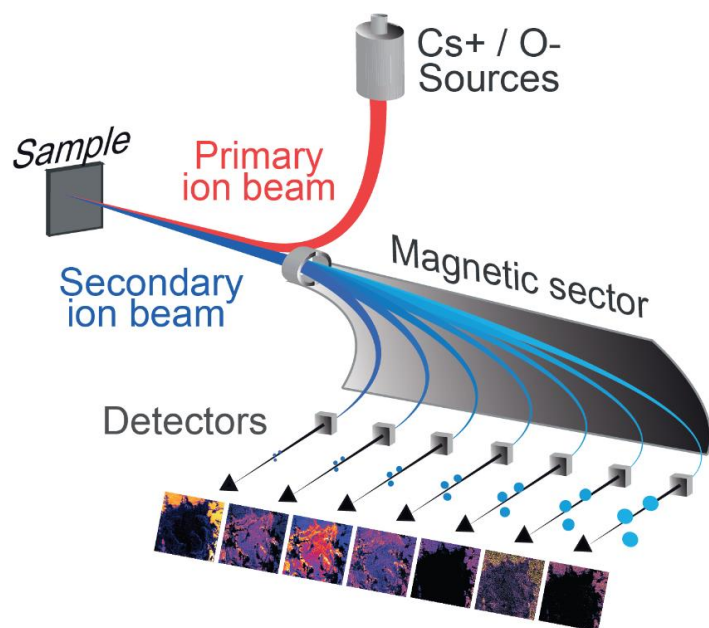
Figure 3.2. The configuration of NanoSIMS features co-axial primary and secondary ion beams. This figure was adapted with a permission from Agui-Gonzalez *et al.*[126]

The static and dynamic SIMS approaches can be distinguished by the primary ion dose. Static SIMS is a surface sensitive technique where the primary ion density is maintained below the static limit. Below that limit, the probability of two ions hitting the same location is low. Generally in static SIMS, the primary ion dose is less than about 10^{13} ions/cm^2, which corresponds to about 1% of the first layer surface impacted by the primary ion.[127]

$$\textbf{Primary ion dose} = \frac{\textbf{I}_\textbf{p}\textbf{t}}{\textbf{A}} \qquad (3.2)$$

Where I_p is the primary ion flux (ions/s)

t is the analysis time (s)

A is the surface area (cm^2)

3.5 ToF-SIMS

Currently, the static SIMS approach has grown dramatically in biology studies, particularly for the detection and visualization of biomolecules. There are three types of mass analyzers used in static SIMS instruments for the separation: a quadrupole, magnetic sector, or ToF spectrometer. Excellent detection limits and mass resolution can be achieved with a magnetic sector spectrometer; but the mass range is limited, generally less than 300 amu. The quadrupole, on the other hand, provides a wide mass range up to 1000 amu, fast scan speed, and ease of

use. The limitation of a quadrupole is poor mass resolution making it hard to separate several ion species with the same nominal mass. The third one, a ToF spectrometer has advantages of high mass resolution (m/Δm > 10.000), high mass range up to several thousand amu, and rapid data acquisition.[128] In general, the features of a ToF analyzer makes it more ideal for the static SIMS technique.
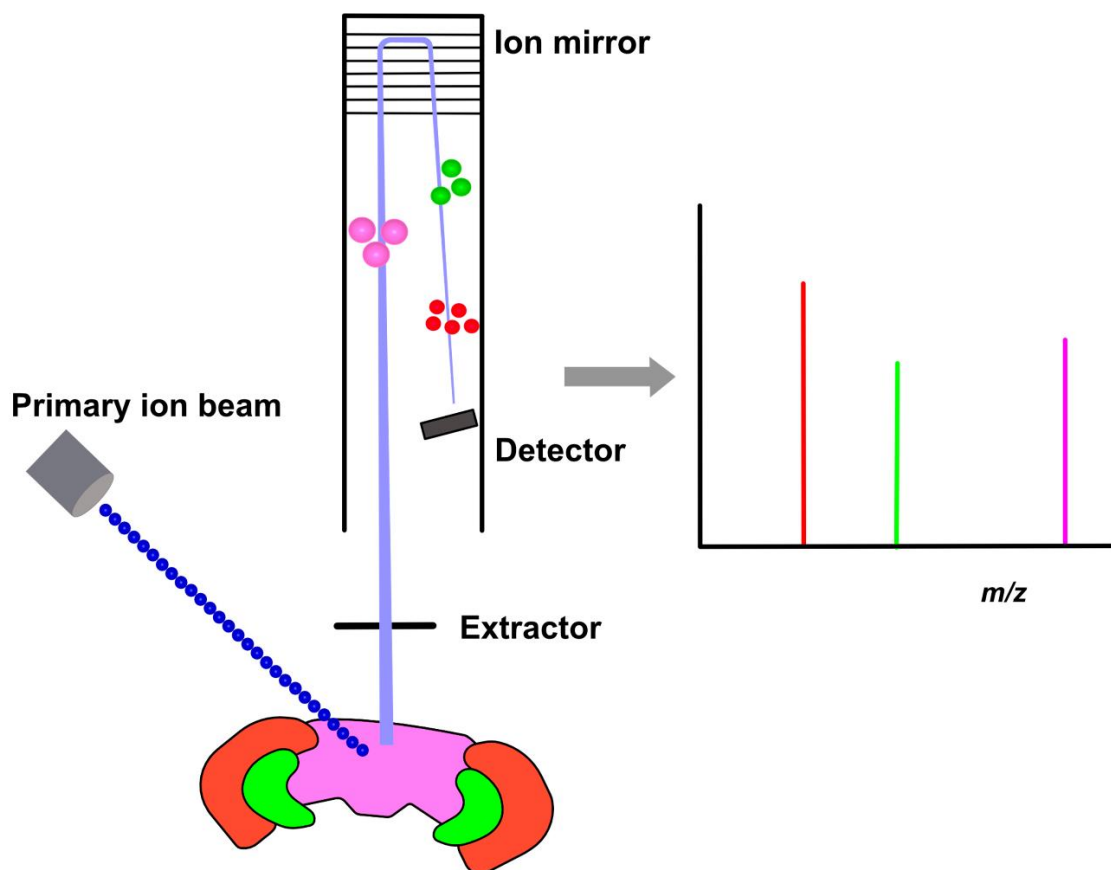
Figure 3.3. Schematic shows the workflow of ToF-SIMS in the imaging mode. A focused primary ion beam ejects secondary ions which are then separated and detected based on their *m/z*. The intensity of each ion for each pixel point can be plotted to generate a chemical image.

The early development of ToF-SIMS was proposed by A Benninghoven and coworkers.[129] A schematic of ToF-SIMS imaging is shown in figure 3.3. ToF-SIMS, however, was not commercialized as an analytical method until the early 1980s. Later, ToF-SIMS evolved into a standard high-resolution surface analysis technique which is useful for elemental and molecular characterization. The introduction of liquid metal ion guns (LMIGs) provided improved lateral resolution for elemental detection (beyond 100 nm).[90, 130] In contrast, the lateral resolution achieved for large molecular species can be several microns.[105, 131] Especially, the ToF analyzer allows one to simultaneously detect and image all

secondary ions in a wide mass range. The difficulty in this technique, however, is to produce a finely timed short-duration primary ion pulse because, in the ToF mass analyzer, a defined start time is required for mass determination based on the flight time of ions. The design of most ToF-SIMS instruments utilizes a pulsed ion beam operating at a low current; thus, this technique is well-suited for analysis of surfaces and soft materials, but not for depth profiling.

The formation of atomic and molecular secondary ions relies on the type and energy of incident primary ions and the nature of the sample. Over the last decades, LMIGs, such as Bi, Au, or Ga, have been introduced to become the ion guns of choice for many ToF-SIMS imaging applications because this can provide submicron-level spot size and can achieve pulses of a few nanoseconds. Unfortunately, most ejected particles are atomic species resulting in a loss of information about the molecular structure of the surface. Hence, the enhancement of the secondary ion yield, particularly of high mass molecules has been a primary challenge for the ToF-SIMS technique. Originally, the first LMIG to be used was the Ga source and then this was adapted to Au, but now the Bi ion sources are preferred due to the improvement of secondary ion yield gained from these sources.[132] Along with the LMIGs, the large cluster C_{60}^+ ion beams were proposed as projectiles which showed potential for characterizing somewhat larger molecules.[92] The C_{60}^+ cluster ion beam containing multiple atoms each having relatively low energy as it impacts the sample surface. The results of these low energy impacts are the reduction of the localized sub-surfaced damage and preservation of molecular structures. Smiley *et al.* illustrated the sputtering of a C_{60}^+ ion beam on an ice film causing the formation of a much wider crater than the Au_3^+ ion beam.[133] The spatial resolution of cluster beams, however, is not good compared to the LMIG sources.[134] More recently, gas cluster ion sources with a cluster size up to several thousand atoms, often Ar_n (n = 500 - 4000), has been designed. Compared to the C_{60}^+ ion beam, the super large Ar cluster beam produces lower impact energy per ion. Importantly, such large cluster ion beams with a spot size of several microns have been used to show a dramatic elevation of the secondary ion yield in the mass range for biological and organic materials.[135] Furthermore, the cluster ion guns are be able to provide efficient sub-micrometer imaging and also 3D molecular depth profiling. 3D imaging in ToF-SIMS can be formed by stacking 2D images acquired at different sample depths.[136-138] As the development of the ion sources is better suited to research studies, the applications of ToF-SIMS will no doubt continue growing rapidly.

3.5.1 ToF mass analyzer

The ToF mass spectrometer separates multiple ions according to their different velocities in a field-free drift path or a flight tube. In Tof-SIMS, a short pulsed primary ion beam bombards the sample surface and induces the formation of secondary ions. The pulse of primary ion beam is the starting point for the time measurement. All secondary ions are then accelerated by an electric field before travelling toward the flight tube. As all secondary ions are given the same kinetic energy, their velocities and therefore the flight time of the ions depends on their masses. When they enter a field-free tube, they are separated according to their velocities before arriving at the detector.

The kinetic energy given to charged particles in an electric field can be described by equation 3.3.

$$\mathbf{E} = \mathbf{qV} \tag{3.3}$$

Here, $\mathbf{E}$ is the kinetic energy, $\mathbf{q}$ is the charge of an ion, and $\mathbf{V}$ is the acceleration potential.

When an ion with mass m and charge q is accelerated by a potential V. The electric potential energy of an ion is converted to kinetic energy E.

$$\mathbf{E} = \frac{1}{2}\mathbf{mv^2} \tag{3.4}$$

Here $\mathbf{m}$ is the mass of the particle and $\mathbf{v}$ is the velocity of the particle.

When an ion travels in a flight tube of known length, L, to the detector, the required time t to pass the distance L is given by the rearrangement of equations 3.3 and 3.4.

$$\mathbf{t} = \frac{\mathbf{L}}{\mathbf{v}} = \frac{\mathbf{L}}{\sqrt{\mathbf{2V}}}\sqrt{\frac{\mathbf{m}}{\mathbf{q}}} \tag{3.5}$$

Equation 3.5 shows the correlation between the arrival time and the mass of an ion. Since the flight time for one ion to reach the detector is proportional to the square root of its mass, lighter ions having higher velocities reach the detector earlier than heavier ions.

The main drawback of the first linear ToF mass analyzer was poor mass resolution because of the broad energy distribution of secondary ions.[139] Indeed, the ions with the same mass were emitted with different initial kinetic energies causing a broadening of the ion packet as it traveled from the sample surface to the detector. The ions with low initial kinetic energy in that case trailed behind the ions with high initial kinetic energy. Another factor also influencing the mass resolution was that the secondary ions were emitted with an angular distribution

from the sample surface. As a result, these ions had a longer flight time. A way developed to improve the mass resolution from the early approach is the use of an ion reflector also called a reflectron or ion mirror. The reflectron helps to correct the initial kinetic energy dispersion of analyzed ions with the same *m/z*. A reflectron, a two-stage ion mirror system, was first invented by Mamyrin and coworkers.[140] The common reflectron consists of a field free drift region, and an ion mirror. As secondary ions enter the mass analyzer, they are accelerated in a potential field and travel toward the field-free region of the spectrometer. At the end of the flight tube, ions inter the reflectron at a slight angle where they are then reflected by the ion mirror, travel back into the field free region at a different angle, and hit the detector. The ion mirror consists of a series of evenly spaced electrode plates generating a strong homogeneous deceleration field followed by a weaker mirror field. As ions with the same *m/z* pass the first deceleration section of the mirror, they slow down, reach to a stop, and then reverse their travel directions to exit the mirror. High kinetic energy ions, and thus having more velocity, penetrate deeper into the mirror than ions with lower energy. High energy ions then catch up to the low energy ions of the same mass until they strike the detector at the same time. The mass resolution m/Δm > 10.000 can be achieved in SIMS performance with a two-stage ion mirror.[128] Most of ion mirrors have a linear electric field. Another variation of the ToF reflectron, which employs non-linear field distribution within the ion mirror, has been introduced.[141] This approach is suitable to apply for system where secondary ions with very large energy spread have to be compensated. This situation can be obtained in the system operating the delayed/pulsed ion extraction or utilizing the secondary ion bunch compression (such as in the J105 instrument). The non-linear field reflectron consists of a large number of equally spaced ring electrodes which create a non-linear electric field to reflect ions. Ions with broad kinetic energies penetrate the mirror with different depths before reversing their directions toward the detector.

3.5.2 ToF-SIMS analysis with the J105

A principle drawback of ToF-SIMS is the requirement of pulsed primary ion beams. The very short pulse of primary ion beams is necessary to maintain good mass resolution. High spatial resolution is only achieved when a long pulse of primary ion operating at low ion current is used. Additionally, the low duty cycle of the pulsed beam consequently leads to long time for analysis. A relatively new approach is found in the J105 ToF-SIMS instrument, which was developed by the

group at the University of Manchester (UK) collaborating with Ionoptika Ltd. (Southampton, UK).[142] A schematic of the instrument is shown in the figure 3.4. The aim of this development was to decouple the mass resolution with the spatial resolution by removing the need to pulse the primary ion beam. The J105 instrument utilizes a continuous primary ion beam combined with a bunched secondary ion stream which enables one to obtain high spatial resolution images with high mass resolution spectra.
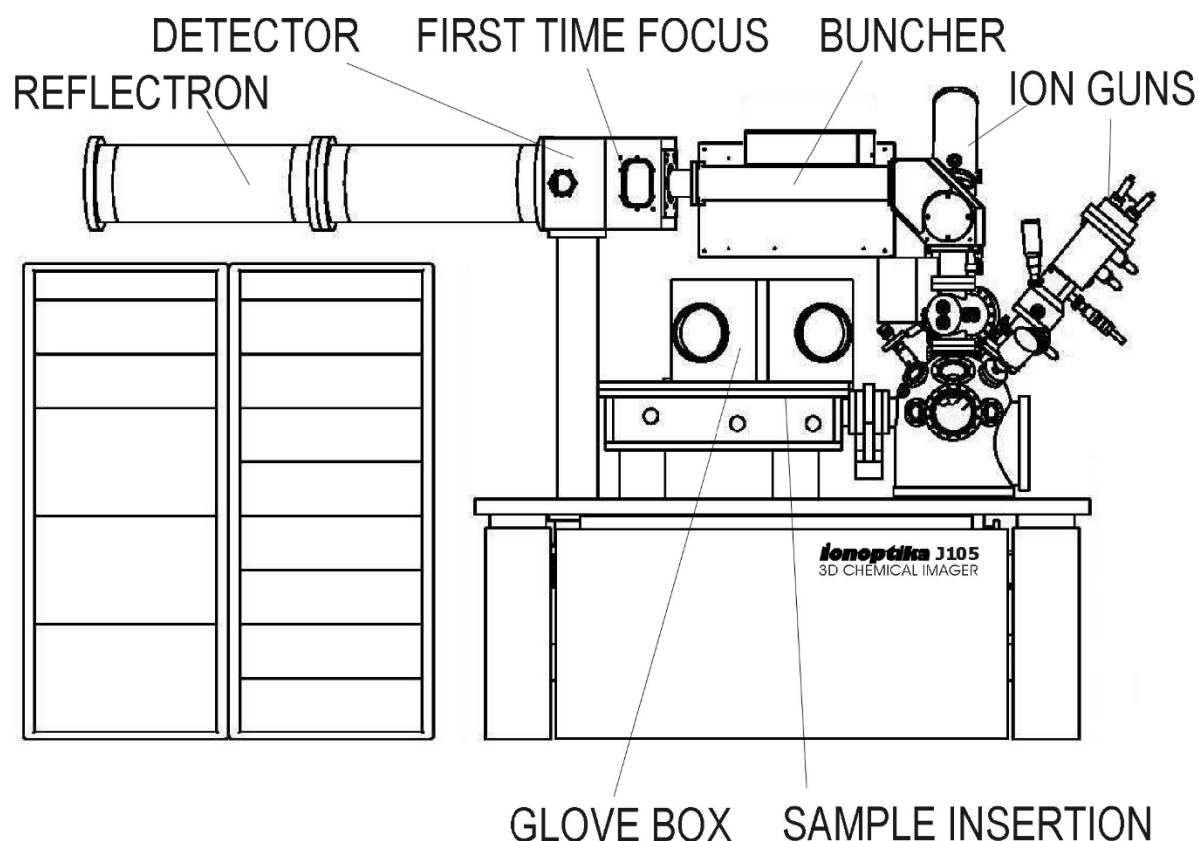
Figure 3.4. Schematic of the J105 3D Chemical Imager. Image is reproduced and adapted with the permission from Fletcher *et al.*[142]

In the J105, a continuous primary ion beam sputters the sample surface which produces a continuous stream of secondary ions. The secondary ions are extracted into a radio frequency-only quadrupole filled with suitable gas (e.g. N_2), where they are collisionally cooled. The ions are then energy filtered by an electrostatic analyzer, thus providing them with a 1 eV energy spread before entering a linear buncher (Figure 3.5). The secondary ions are collected in the buncher and subsequently accelerated into the flight tube at the same time; thereby they are condensed in toa narrow spot at a time focus at the entrance of the reflectron. The buncher consists of several plates applied an acceleration field that varies from 6

keV on the plates at the entrance to 0.5 keV on the plates at the exit. With this application of the buncher, the ions at the back of the buncher are able to catch up with the ions in the front. These ions, however, have a large energy spread (about 6 keV) which would be a problem for a conventional ToF analyzer. The J105 utilizes a non-linear field ToF reflectron which contains a short field free region and is filled with reflectron plates. Thus, ions are separated due to their mass to charge ratios, but not their energy. The mass resolution is dependent on the buncher performance and decoupled with the secondary ion formation. The current J105 set-up can achieve a mass resolution of $m/\Delta m \sim 10.000$ and a mass accuracy of 5 ppm.
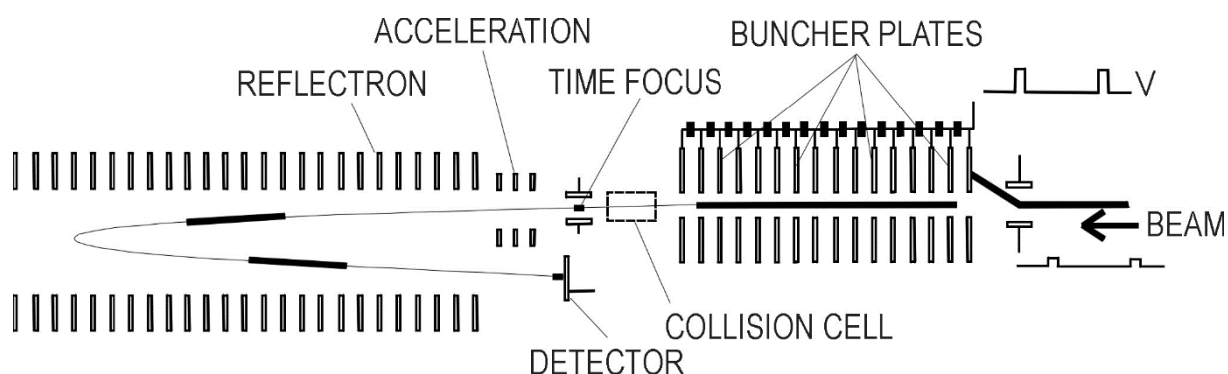
Figure 3.5. The configuration of the buncher and reflectron on the J105. Image is reproduced and adapted with the permission from Fletcher *et al.*[142]

The design of the J105 is especially optimal for biological analysis. The J105 is equipped with large-cluster primary ion beams including C_{60}^+, Ar_n^+, or $(CO_2)_n^+$ all giving high yield for intact biomolecules. Furthermore, the J105 can be cooled down to about 100 K using liquid nitrogen which allows one to perform analysis on frozen hydrated samples. The glove box on the top of the sample insertion can be filled with inert gas (e.g. Ar) to prevent the frosting of frozen samples.

MS/MS can be performed with the J105 instrument. For MS/MS analysis, after the buncher, the ions travel to a collision cell filled with a suitable gas (e.g. He, N_2, or Ar) where the ions are fragmented. Since the collision cell is placed after the buncher, the collision energies are in the range of 0.5-6 keV. The collisions occur in the short field free region; and hence both parent and daughter ions travel further with the same velocity. The ions of interest are selected by a timed ion gate before passing to the ToF analyzer.

3.5.3 ToF-SIMS improvement for biological analysis

All biological functions of living organisms depend on properties and behaviors of biological machines, which are large molecules including lipids, proteins, nucleic acids, carbohydrates, and much more. Several areas of biological sciences have been attracted to study the structures, compositions, and functions of these biological machines. In recent years, ToF-SIMS has been increasingly applied to visualize and characterize the lateral distribution of specific species in biological tissues and cells. The advantages of this technique include sub-micrometer resolution, labeling-free approach, and an ability to obtain both 2D and 3D images. Until recently, ToF-SIMS imaging had poor secondary ion production owing to the traditional Ga^+ or In^+ LMIGs used. The introduction of cluster LMIGs and large cluster ion beams have led to huge improvements in secondary ion yields, especially for high-mass ions, making this approach more well-suited for studies of biological applications on various samples, such as tissues, cells, and bacteria.

Nowadays, the need to localize and identify biomolecules in single cells has become more important in life science for better understanding of biological processes.[143, 144] The surface sensitivity of ToF-SIMS makes it well-suited for the analysis of the cell membranes. One of the first applications of ToF-SIMS in single cell molecular imaging was reported by Winograd and Ewing.[145] In that report, a Ga^+ LMIG was used to image molecular species across the surface of the single cell organism *Paramecium*. Later, ToF-SIMS equipped with an In^+ primary ion beam revealed alterations in lipid composition consistent with high and low curvature lipids during *Tetrahymena* mating.[146] These changes occurred at the conjugation site where a fusion pore was formed to pass the micronuclei between the cells. The fusion site between two cells contained a reduction of low curvature lipids PCs (*m/z* 184) and an elevation of high curvature lipid 2-aminoethylphosphonolipid (*m/z* 126). Unfortunately, the use of a monoatomic ion beam in single cell imaging allows one to only identify the fragments of lipid species. As mentioned, to increase secondary ion yield of high-mass molecules, the Ga^+ or In^+ sources have now been largely replaced with cluster ion beams. This is highlighted in the recent work of Kollmer *et al.* where secondary ion yields gained from cluster beams, such as Au_3^+, Bi_3^+, and C_{60}^+, were shown to be significantly increased compared to Ga^+.[147] The potential benefits of cluster beams in applications to biological science are significant and wide-reaching.[148-150]

Lipidomic analysis has gained the attractions of scientists because of the important roles of lipids in many cellular processes. Lipids from brain tissues, cell membranes, heart, liver, or muscle have been studied most extensively with ToF-SIMS.[151-157] In addition, the dysregulation of lipid mechanisms has been shown to be involved in many diseases and mental disorders, such as cardiovascular disease,[157] Alzheimer's disease,[158] and cancer.[159, 160] Understanding of lipid distributions in the brain tissues can give insights into to the underlying processes of these diseases. ToF-SIMS imaging using Bi_3^+ cluster ions has been used to determine the cholesterol distributions in Alzheimer disease human brains. The results revealed an elevation of cholesterol levels in the cerebral cortex of Alzheimer disease patients.[161] In addition, a Bi cluster ion source on a ToF-SIMS was applied further to map lipid localizations in nonalcoholic fatty liver disease.[79] They found the elevation of TAGs, DAGs, MAGs, and FAs together with the depletion of vitamin E in the liver tissue compared to control. Myocardial infarction, also a term used for a heart attack, occurs due to the reduction of blood flow to a part of the heart; after which the heart muscle is damaged because of lack of oxygen. The lipid distribution in the infarcted region of mouse hearts was probed using Ar_{4000}^+ GCIB ToF-SIMS.[157] A depletion of PI levels and the increase in DAG signals was observed in the infarcted regions of mouse heart tissues compared to normal regions. Interestingly, the specific PI species are accumulated in the border of infarcted and non-infarcted regions. In addition to lipid changes induced by diseases, several medications have been reported to have impacts on lipid levels. A recent work from Phan *et al.* used GCIB ToF-SIMS to investigate the effects of methylphenidate on the distribution and composition of lipids in the fly brain.[153] Methylphenidate is a stimulant medication for treatment of attention deficit hyperactivity disorder. The significant decrease in the abundance of PC species was obtained after methylphenidate administration, whereas methylphenidate caused the elevation of PE and PI levels in the fly brain. Furthermore, stable isotopes can be probed within the cells with ToF-SIMS to determine the uptake of specific substances or track the chemical transformations through biological synthesis. One example is the use of a LMIG and GCIB to track the incorporation of deuterated fatty acids and lipid turnover from these fatty acids into the plasma membrane of cells (as seen in paper II).

Current ToF-SIMS methods provide chemical information not only within the uppermost layers of the exposed surface but also as a function of depth. As mentioned earlier in this chapter, the introduction of the ion cluster beams has

brought more chances for new applications of 3D molecular imaging and molecular depth profiling for ToF-SIMS analysis.[162] The 3D biomolecular ToF-SIMS imaging of a single cells, *Xenopus laevis oocytes,* was reported by Fletcher *et al.*[136] In this paper, the J105 ToF-SIMS instrument was equipped with a continuous C_{60} primary ion beam to characterize chemical changes in three dimensions of a single cell. A wide range of lipid species including cholesterol, FAs, DAGs, and PCs were observed through the sample with a predicted erosion depth of 175 μm. The most recent study from Dimovska Nilsson *et al.* characterized the lipid composition in the envelops of Escherichia coli mutants having impaired plasmid transfer ability to share the DNA in antibiotic resistant bacteria.[163] Differences in the chemical composition, especially FAs, in the surface of different bacterial strains were obtained using ToF-SIMS with a $(CO_2)_{6000}^+$ GCIB. Interestingly, the GCIB in this study provided significant signals from higher mass species up to several thousand *m/z*, such as intact lipid A (*m/z* 1796) along with other species at *m/z* 1820 and 2428.

In general, ToF-SIMS brings several opportunities for biological applications to the MSI field. In this thesis, ToF-SIMS imaging has been applied to investigate the changes in lipids induced by drugs in both brain tissues and cells samples.

Chapter 4

ToF-SIMS imaging for biological applications

Owing to several practical and ethical obstacles, experiments using humans in biomedical sciences are severely limited. Thus, there is a need to find simpler biological model systems to answer biologically related questions. Animal models, such as rat, mice, invertebrates or cells, are commonly used. ToF-SIMS analysis of animal model organisms requires simple sample preparation. However, further investigations for sample preparation procedures are crucial to improve the yields of molecular species. The first part of this chapter discusses the model organisms used for biological research. Later, sample preparation for ToF-SIMS experiments and data analysis are also described.

4.1   Short survey of the field

When MALDI imaging was first introduced in 1997, this technique became an important breakthrough in the field of MSI.[100] MALDI is capable of probing large biomolecules with several thousand Da like peptides and proteins. MALDI has emerged as a great tool to study single neurons,[164] as well as brain sections.[165] Furthermore, there is a rapid growth of the current attention in the MALDI technique focusing on several diseases including Alzheimer's disease,[31, 166] Parkinson's disease,[167] and infectious disease.[168] In the MALDI technique, a thin layer of an organic matrix is coated onto the surface of the sample to improve the ionization efficiency. The requirement of the addition of a chemical matrix somewhat limits the spatial resolution and mass range below 500 Da. SIMS imaging, on another hand, provides higher spatial resolution over a lower mass range, usually below 1000 Da. The surface analysis SIMS technique has been particularly attractive for imaging of tissues and single cells, even at submicron scale.[145, 169] Recently, several new designs of SIMS have improved its application in biological science. One design, the J105 instrument from IonOptika, includes a novel ToF spectrometer equipped with a continuous huge cluster ion beam which increases the ion yields for large biomolecules. Moreover, MS/MS imaging is possible with the J105.

Another MSI approach, desorption electrospray ionization (DESI), allows the surface imaging of biological samples in the ambient environment without any chemical treatment.[170, 171] In DESI experiments, the wetted sample surface is impacted with charged droplets of solvents leading to the desorption of secondary droplets.[172] Although the sensitivity and spatial resolution for most DESI experiments appear to be poorer than what is achieved by MALDI and SIMS, the imaging of wet samples is possible in DESI. The capability of DESI-MS to map lipidomic profiles in rat brain tissue has been demonstrated with spatial resolution of less than 500 μm.[171]

FT-ICR MS offers both high mass resolution and mass accuracy for biomolecular identification.[173] Currently, a new instrument has been developed which combines the high spatial resolution ToF-SIMS with the high mass-resolving power FT-ICR instrument. The ions generated in the ToF-SIMS apparatus are transported to the analyzer of an FT-ICR instrument to gain high spatial resolution images with high mass resolution spectra. The Heeren group reported the first combination of an C_{60} ion source with an FT-ICR MS to image the mouse brain tissue.[174] In this work, the authors showed examples of mass measurement accuracy below 1 part-per-million, and mass resolving power in excess of 100.000, as well as spatial resolution of 40 μm. The practical limitation of FT-ICR MS instruments, however, is their slow acquisition rates. Another powerful approach called the 3D OrbiSIMS provides high speed imaging while maintains the high mass-resolving power and high mass accuracy.[175] The 3D OrbiSIMS is a hybrid instrument consisting of TOF.SIMS 5 (ION-TOF GmbH, Germany) and a Q Exactive HF Orbitrap (Thermo Fisher Scientific, Germany). The high-speed imaging can be achieved by ToF spectrometer while the Orbitrap MS provides good mass resolving power of 240.000 at m/z 200 and a mass accuracy of less than 2 ppm. It is configured with dual ion beams (Ar^n and Bi^n) and dual analyzers (ToF and orbitrap) which offers surface analysis, depth profiling, and 2D and 3D imaging. The 3D OrbiSIMS has been applied in biological imaging to probe the distribution of several biomolecules. In addition, the visualization of 3D images at subcellular resolution is possible with the 3D OrbiSIMS system. An analysis of biological samples at frozen-hydrated state can be performed due to a cryogenic sample holder.

4.2 Biological models

In the early days of molecular biology, the simplest organism like bacteria and bacteriophages were chosen to study various different molecular mechanisms including the replication, transcription, protein synthesis and gene activity control. Later, in order to accumulate more complicated knowledge, biological research required more complex systems such as *Caenorhabdtis elegans*, *Drosophila melanogaster*, zebra fish, and rodents. These models have had a huge contribution for fundamental biological and clinical research. Two different models, the fruit fly *Drosophila melanogaster* and pheochromocytoma or PC12 cells have been used in this thesis to investigate the changes in lipid distribution and composition induced by drug treatments.

4.2.1 *Drosophila melanogaster*

Use of the model *Drosophila melanogaster*, the fruit fly, has led to several major breakthroughs in genetics. It has become a common choice of model organism in biomedical research for over a century. The fruit fly is inexpensive and easy to maintain in the lab. Moreover, it has a short life cycle which can readily be produced in large numbers for experiments. Normally, 9-10 days on average is required for the development process from a fertilized egg to an adult at 25°C (Figure 4.1). The fly undergoes four developmental stages: the embryo, larva, pupa, and adult. Upon fertilization, the embryo grows in the egg around one day at 25°C, followed by three larval stages termed the first, second, and third instar. The young small larvae have to shed their entire outer skins to grow to a larger size. During this stage, larvae spend their time eating and their growth take places in about 4 days. The third instar larvae crawl out of the food medium onto a dry place, cease moving, and then pupate. The larvae undergo a 4-day-long metamorphosis (at 25°C) in the puparia, after which the adults emerge. The duration of the fly life cycle depends greatly on temperature, being more rapid at high temperature.

When the *Drosophila* genome was fully sequenced in 2000,[176] it was found out that many basic biological, physiological, and neurological properties between *Drosophila* and mammal are conserved. Reiter and co-workers reported that approximately 77% of genes involved in human diseases have matches in the fly genome;[177] thus offering several advantages for investigation of the molecular and cellular mechanisms underlying human diseases with fly models. For instance, several fly models have been developed to study the function of specific

genes which involve complex diseases such as Parkinson's, Alzheimer's, or Huntington's diseases.[178-182] In addition, the fruit fly is an excellent model in genetic analysis which helps one to understand the development, function, and plasticity of neural networks.[183]
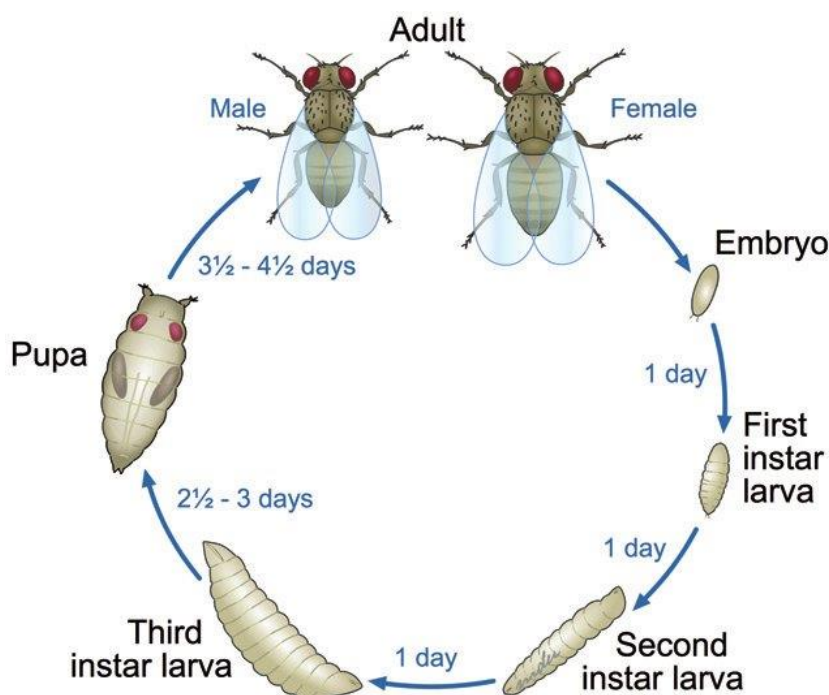

Figure 4.1. A schematic of *Drosophila* life cycle. The fly development includes various stages: the embryo, larva, pupa, and adult. The figure is modified from Ong *et al.* [184]

The *Drosophila* embryo provides a useful system for the study of numerous cellular processes including cell-to-cell communication, cell division, gene expression, and cell death. Disruption of these processes can lead to severe problems of the embryo including deformities, infertility, or death. The mystery of brain function, such as cognition and behavior, is the main drive for neuroscience research today. Studies with fruit flies have provided insights about the development of the nervous system, ion channel function, axon function, synaptic transmission, learning and memory, and neural diseases. The nervous system of larvae and adult flies contains a relatively small number of neurons, but displays the same brain functions as vertebrates at the molecular, cellular, and behaviors levels.[185] The larval brain comprises about 10 000-15 000 neurons, while the nervous system of an adult fly is more complex with 100 000 neurons.[186-188] The larval brain contains various neurotransmitters including octopamine, dopamine, serotonin, tyramine, glutamate, and acetylcholine.[189-191] To study the regulation of amine release at an intact neuron, Majdi *et al.* probed

the release of octopamine in the *Drosophila* larva by amperometry.[192] Similar to the larval brain, the brain of an adult fly uses neurotransmitters like dopamine, GABA, glutamate, acetylcholine, serotonin, histamine, and octopamine to communicate between neurons.[190, 191, 193] The Ewing group, described real-time neurochemical measurements in *Drosophila* in which the uptake of exogeneous applied dopamine was quantified using fast scan cyclic voltametry.[194]

Monoamine transporters in the brain are the main targets for psychostimulants to regulate the extracellular levels of monoamines, such as dopamine. Several studies on the effect of psychostimulant action on the dopamine transporter in the fly have been reported. For instance, Berglund *et al.* studied the effects of methylphenidate on dopamine uptake during direct bath application of cocaine onto the fly central nervous system.[195] They found that the dopamine transporter in the fly is inhibited by oral administration of methylphenidate, thus inhibiting the action of directly applied cocaine. In addition to neurochemical research, the fruit fly provides an ideal model system to study lipid metabolism induced by diseases and drugs.[196] Compared with mammals, *Drosophila* shares the basic metabolic pathways and signaling pathways involved in lipid metabolism. One example is the alteration in lipid distribution and composition in the central fly brain obtained after cocaine and methylphenidate administration (paper I and III).

4.2.2 PC12 cells

The rat pheochromocytoma (PC12) cell line was originally isolated and cultured from a tumor in the adrenal medulla of a rat in 1976 in the lab of L. Greene.[197] An image of a PC12 from transmission electron microscopy (TEM) is shown in figure 4.2. Since its initial description, the PC12 cell line has been widely used for studies of neuronal development and function.[198, 199] PC12 cells are capable of differentiation into a neuronal phenotype by responding to nerve growth factor.[197, 200] PC12 cells have large dense core vesicles containing catecholamines, such as dopamine and norepinephrine, as well as smaller synaptic vesicle-like microvesicles containing acetylcholine.[201, 202] Thus, PC12 cells offer many advantages for studying exocytosis and related processes.[198, 203] Furthermore, PC12 cells represent an important model for lipidomics studies, particularly lipid changes in the cell membrane during several different processes or drug treatments. For instance, organic pollutants can induce changes in lipid metabolism in PC12 cells.[204] Cholesterol has been shown to regulate dopamine release during exocytosis in PC12 cells.[205] Corsetto *et al.* showed that apoptosis in PC12 cells induced by manganese is associated with the changes in lipid

composition.[206] In paper II, the synthesis of membrane lipids in PC12 from fatty acids was investigated by using ToF-SIMS imaging. The use of isotopic-labelled fatty acids as lipid precursors resulted in spatial information of converted fatty acids and lipid turnover. Especially, the relative abundance of lipids incorporated from isotopic fatty acids was also measured based on the isotope peaks from ToF-SIMS spectra.
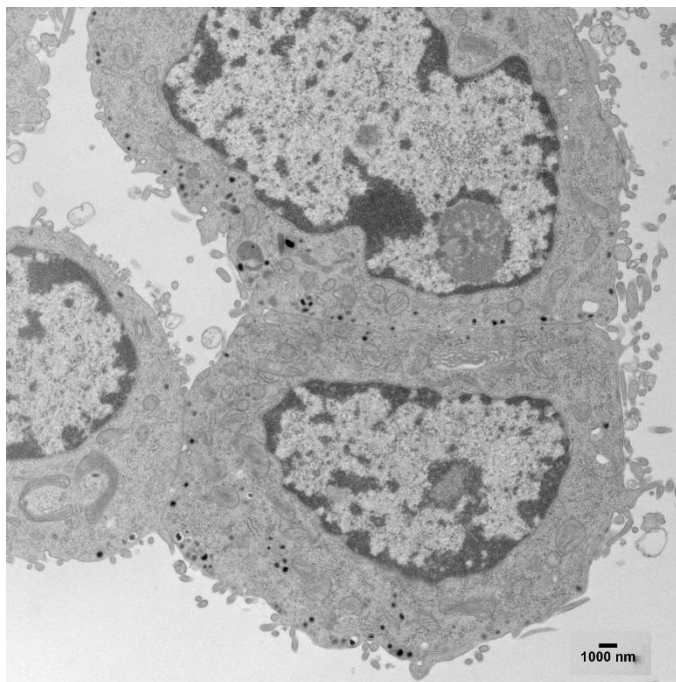
Figure 4.1. TEM micrograph of PC12 cells.

4.3 Sample preparation for ToF-SIMS

Although there is no requirement of any preliminary treatments of the sample (e.g. coated by matrix, salt, or metal) in ToF-SIMS imaging, the preparation of biological samples is still important to preserve the morphological structure of the sample and the original chemical location of the analyzed species. There are three common sample preparation methods for SIMS imaging: freeze-dried, frozen hydrated, and chemical fixation methods.

The simplest method for analysis under vacuum is freeze-drying. Before samples are dried, cryofixation is commonly employed to preserve the sample integrity. Samples are plunged quickly into a cryogenic liquid, such as liquid propane (85 K) or ethane (89 K). The cryogen has a low boiling point and high thermal conductivity to cool the sample fast enough to transition water to amorphous ice; thereby, the formation of ice crystals causing molecular displacement and the damage of sample structure is prevented. After cryofixation,

frozen samples are typically embedded with specific materials (e.g. optimum temperature cutting, gelatin, or ice) for sectioning into thin slices using a cryomicrotome.[207] Sample sections are commonly thaw-mounted onto a conductive substrate, such as an indium tin oxide coated glass slides or silicon wafers. The frozen samples are then freeze-dried under vacuum to remove water by sublimation. After drying, the nonvolatile substances like salts are crystalized on the sample surface which causes severe problems during ToF-SIMS analysis. The accumulation of salts on the sample surface must be prevented or salts removed to give better signals of analyzed molecules. Wu and co-workers found that the majority of interfering substances like salts and cell culture components were washed away by using ammonium acetate ($CH_3CO_2NH_4$) before cryofixation.[208] Due to the volatility of ammonium acetate, no residue remains after the drying procedure. Similarly, the volatile salt, ammonium formate (NH_4HCOO), can also be used for the same purpose.[169] Another drawback of the freeze-dried method is the relocation of species owing to the loss of water during the drying process. For instance, changes in distribution of cholesterol have been observed in brain tissue samples after freeze drying and the migration of DAG species has been reported in the fly brain .[209-211]

Chandra et al. described frozen-hydrated sample preparation for cell analysis with SIMS to eliminate the rearrangement of molecules and preserve sample morphology.[212, 213] Instead of freeze-drying, sample sections were kept frozen throughout the analysis. Performing the frozen hydrated analysis showed the enhancement of the signals for biomolecular species.[211, 214] The formation of ice condensation on the sample surface, which occurs during sample transfer, was a typical problem of this method. Etching techniques, such as freeze etching and C_{60}^+ etching, have been utilized to remove the condensation layers.[215] Another way to avoid the condensation contamination has been via the freeze-fracturing technique where cells are sandwiched between two pieces of silicon and then frozen.[216, 217] The frozen sandwich can then be fractured to expose cells for analysis.

Finally, chemical fixation can also be used. Due to the fact that chemical fixatives can react with the molecules or change the molecular structures in the sample, chemical fixation should be avoided for sample preparation in ToF-SIMS analysis.[218] This method, however, is routinely utilized for NanoSIMS analysis, for instance glutaraldehyde can be used for protein fixation and osmium tetroxide for lipid fixation.[219]

Various methods for ToF-SIMS sample preparation have been developed to improve the molecular ion yield during sputtering. Matrix enhanced-SIMS, where a thin layer of MALDI matrix is coated onto the sample surface, can be used to gain improvement in the ionization efficiency.[220] The disadvantage, however, is the rearrangement of molecules during the matrix deposition. Moreover, the size of the matrix crystal is larger than the beam size leading to the loss in spatial resolution. In contrast to matrix enhanced-SIMS which typically uses organic matrices, another variant called metal-assisted SIMS utilizes metal deposition.[169, 221] Nonetheless, the enhancement in secondary ion yields is observed only for some specific species which form adduct ions with metals. Treatment with ammonia induces an increase in signal intensity of sulfatides and ceramides in rat brain tissue samples owing to the reduction of the cholesterol precipitation on the sample surface. Trifluoroacetic acid treatment is another method that can be used to reduce signal intensity of cholesterol, thus increasing the intensity of lipid molecules.[222, 223]

4.4   Principal components analysis (PCA)

A data set of spectra generated from ToF-SIMS is usually large in size and rich in information containing perhaps hundreds to thousands of peaks. When one analyzes biological materials, the ion yields for intact biomolecules is lower than the signal intensity of fragments. Extracting the relevant biological information from a complex spectrum is challenging. A wide variety of multivariate analysis (MVA) techniques, including principal components analysis (PCA), maximum autocorrelation factor, or partial least squares regression, have been applied to ToF-SIMS data to simplify the data analysis.[224, 225] Among these methods, PCA is the most commonly applied MVA technique. PCA is a useful method to simplify the data with a minimal loss of information.[226] PCA translates a large data set into a number of principal components where the first principal component (PC1) captures the most variance in the data set. The relationships between the variables (*m/z* value in ToF-SIMS spectra) are displayed in score plots, while corresponding loading plots represent which variables (peaks) contribute to the separation seen in the score plot.[227]

It is crucial to use an appropriate data pretreatment approach prior to PCA to get better separation. The main purpose of data pretreatment methods is to convert data to a different scale (e.g. logarithmic scale) to focus on the significantly relevant information and reduce the artefacts (e.g. measurement noise or

differences due to instrumentation/topography). Data preprocessing includes peak selection, data normalization, and suitable scaling methods. Peak selection is the first step to make the set of peaks to run PCA. It is more common for one to select the peaks from the region of interest to remove the interferences from noise or background. After peak selection, data binning can be used owing to the large number of peaks. The data set is then normalized by dividing the intensity of each peak to a scalar value (e.g. normalization to the total intensity of selected peaks or the total secondary ion intensity). The goal of normalization is to minimize variations caused by sample charging, instrumental conditions, or topography.

Data scaling is a critical step in PCA which influences the separation of the valuable information from noise. In the scaling method, each variable (peak) is divided by the scaling factor. As an example, autoscaling, also known as unit variance scaling, uses the standard deviation as a scaling factor. Unit variance is probably the most common scaling method since all variables become equally important. Pareto scaling scales the data by dividing by the square root of the standard deviation for the variable. Pareto scaling helps to reduce the relative importance of intense peaks and enhance the contribution of the weaker peaks that might be biologically relevant.

The software SIMCA (Umetrix, Sweden) was used in this thesis for PCA on ToF-SIMS spectra. This software was used to extract the changes in intact biomolecules in fly brains owing to drug exposures (papers I, III, and IV). Additionally, image PCA on ToF-SIMS images of fly brain sections was carried out on MatLab (The MathWorks Inc.) to identify the alteration of lipid distributions shown in paper I.

Chapter 5

Summary of papers

The work in this thesis demonstrates the successful applications of ToF-SIMS imaging in biological research to directly study lipids in tissues and cells. Owing to the use of cluster ion sources and GCIBs, the ion yields were enhanced opening new opportunities to expand the application potential of ToF-SIMS. In this work, both cells and tissues have been analyzed by using either the ION.TOF 5 with a Bi-cluster source or a newer instrument design, the IonOptika J105, equipped with a high energy GCIB. The signals of high-mass intact lipids have been improved as cluster ion beams, especially GCIB, were employed.

In **paper I**, ToF-SIMS imaging was applied to study the effects of psychostimulants like cocaine and methylphenidate (MPH) on the lipids in the brain of the fruit fly *Drosophila melanogaster*. Cocaine and MPH share some similar mechanisms of action in the brain by blocking dopamine transporters leading to the elevation of the extracellular dopamine. Although producing similar dopamine-elevating effects, they have different impacts on cognitive performance. Long-term cocaine use causes a wide range of cognitive deficits, particularly in memory, learning, attention, executive functions, and language. MPH, on the other hand, appears to enhance the cognition performance. The neurochemical actions of cocaine and MPH can lead to the alteration of the cellular activities in the brain associated with the disruption in lipid metabolism. The application of a high energy gas cluster ion beam (a 40 keV Ar_{4000}^+ GCIB) as an ion source in the ToF-SIMS technique provides great advantages to image intact lipids and obtain detailed spatial molecular information inside the fly brain after exposure to cocaine and MPH. Male flies were fed with yeast paste food supplemented with cocaine or MPH for three days. After treatment, fly heads were embedded in gelatin and then cryo-sectioned using a microtome. The samples were analyzed using the frozen-hydrated sample preparation approach with the J105 instrument. Principle component analysis (PCA) was applied to the images to elucidate the differences in lipid distribution after cocaine treatment. The results show that cocaine treatment induces the distributional changes of various different lipid species in fly brain sections. To be more specific, PC species are more dominant in the central region of the control fly brain, whereas

cocaine causes the spreading of the same species in the entire brain. Alternatively, PE and PI species are more concentrated in the central brain after cocaine administration. Specific lipid molecules that change significantly in PCA were selected and their relative abundances were then calculated. The results reveal that cocaine and MPH display opposite effects on the lipid composition in the central area of the fly brain. Particularly, repeated cocaine use causes significant upregulation of phosphatidylcholine (PCs) levels, whereas a downregulated trend for PC levels is observed in the fly brain after MPH administration. The total abundance of phosphatidylethanolamine (PE) and phosphatidylinositol (PI) species is depleted following cocaine. In contrast, MPH increases the total levels of the same species. It is possible that the consequence of the opposite alterations in lipid composition in the central fly brain induced by cocaine and MPH is an impairment or enhancement in cognitive performance, respectively.

Impairments in cognitive performance, however, are known to still persist following cocaine removal. Thus, I hypothesized that the changes in brain lipids might be an important factor for the negative impacts of cocaine on cognitive function. Therefore, ToF-SIMS imaging was used to test whether the alterations in the lipid composition induced by cocaine exposure are reversed after the removal of cocaine or cocaine administration followed by MPH treatment. The results are presented in **paper III**. As mentioned in paper I, male flies were fed with yeast paste food containing cocaine for three days. The flies were then either fed with normal yeast paste food or food supplemented with MPH for another three days. The samples were cryo-sectioned and then freeze-dried for ToF-SIMS analysis. Experiments were performed using the J105 instrument with a 40 keV $(CO_2)_{6000}^+$ GCIB as a primary ion beam. In this work, PCA on ToF-SIMS spectra was used to identify the lipid changes after drug treatments compared to control flies. Interestingly, cocaine removal and cocaine treatment followed by MPH are observed to partially rescue the alteration of lipid composition in the brain induced by cocaine. In detail, cocaine administration leads to the elevation of PC abundance in the central region of the fly brain. Cocaine removal seems to lead to recovery of the effects of cocaine on PC levels, whereas MPH treatment after cocaine induces further depletion of PC levels compared to the control brains. Both strategies lead to a partial recovery of the alteration of TAG concentration caused by cocaine. Alternatively, cocaine causes a significant reduction in total PE and PI levels and these changes are not observed to be rescued by cocaine

removal and MPH treatment. Although cocaine removal and MPH treatment does not completely reverse the effects of cocaine on lipid changes in the fly brain, these strategies still have positive impacts on the brain lipid recovery induced by cocaine action. All together, I suggest that lipid treatment may open up new opportunities to improve the cognitive impairments caused by repeated cocaine use.

In **paper II,** another application of ToF-SIMS for studying of lipid synthesis was investigated. In this work, the deuterated substrates of α-linolenic acid FA(18:3) and linoleic acid FA (18:2) were used to identify the incorporation of fatty acids and lipid turnover in the plasma membrane of cells. Both the omega-3 fatty acid, α-linolenic acid, and linoleic acid, an omega-6 fatty acid, are long chain polyunsaturated fatty acids (PUFAs) which are not synthesized in human body. Both omega-3 and -6 fatty acids have been shown to be useful supplements for treatment against neurodegenerative diseases, cardiovascular diseases, as well as cognitive impairment. They are precursors in the biosynthesis of longer chain PUFAs and lipids. Studying the incorporation of these fatty acids and their lipid turnover into the cell membrane might give insights into the relation of lipids and their positive benefits. In this work, PC12 cells were incubated with deuterated omega-3 and -6 fatty acids for one day. Lipid information was obtained by using a Bi-cluster ion beam (TOF.SIMS 5) and a GCIB ion beam (J105). The Bi-cluster beam provides good spatial information for isotopic fatty acids in the plasma membranes of single cells, whereas the GCIB enhances the signal intensity of lipid turnover from these fatty acids. As expected, the results show that deuterium-labelled omega-3 and -6 fatty acids are accumulated in the cell membrane after incubation. As these are absorbed into the cell, these fatty acids are converted into the longer-chain PUFAs with 20 and 22 carbons via the fatty acid metabolic pathways. Using ToF-SIMS I was also able to show that these fatty acids and their converted products are incorporated into PC, PE, and PI species. Omega-3 fatty acids (with 3 double bonds) and their conversion products (with 3 or 5 double bonds) are incorporated into lipids with 3, 5, or 6 double bonds. Similarly, omega-6 fatty acids (with 2 double bonds) and their conversion products (with 2 or 4 double bonds) participate in the lipid synthesis process to generate lipid species containing 2 or 4 double bonds. Interestingly, the relative quantification of lipid species showed that the accumulation of omega-3 fatty acid in the plasma membrane of the cell is higher than omega-6 fatty acid after

incubation. The relative amount of lipids incorporated from omega-3 fatty acids is also higher than those from omega-3 fatty acids. These findings are important to understand lipid metabolism in the cell and cell membrane and suggest that specific lipids are involved in protection against brain aging as well as having positive impacts on cognitive impairment.

Zinc is an essential trace element which plays an important role in brain function and cognition development. Several reports have demonstrated that a lack of zinc causes the impairments in cognitive performance, especially learning and memory. Therefore, in **paper IV**, the impact of zinc deficiency on the brain lipids in the fly was investigated using the TOF.SIMS 5 instrument (IONTOF GmbH) equipped with a Bi-cluster ion beam. In this study, fertilized fly eggs were collected and the new-born larvae were fed with standard cornmeal food with the removal of zinc. Male adults were selected for further ToF-SIMS experiments. Prior to ToF-SIMS analysis, inductively coupled plasma mass spectrometry (ICP-MS) was performed to quantify the zinc concentration in control and zinc-deficient larvae and adult flies. The results show that the zinc level in larvae with dietary zinc deficiency is about 70% lower than that in control larvae. The concentration of zinc in fly heads, on the other hand, is not significantly different between the control and zinc-deficient groups. The application of PCA to the ToF-SIMS spectra in the lipid region (m/z 650-900) shows significant differences in lipid species in the central brains of flies treated with zinc deficient food compared to controls. The elevation of PC and PI species is observed after zinc deficient diet, whereas a lack of zinc causes the depletion of PE species. The effects of zinc deficiency on lipid levels in the fly brain are similar to what is observed after cocaine administration. Both cocaine and zinc deficiency induce an elevation in PC and a reduction of total PE levels. Taken together, the observed alterations in levels of lipid species, especially PCs and PEs, might be related to the loss in cognitive performance in the brain.

Chapter 6

Concluding remarks and future outlook

ToF-SIMS is a highly sensitive surface technique which is capable of surface chemical mapping and identification of molecular information. For many years, the application of ToF-SIMS imaging was mainly focused on inorganic materials, especially in semiconductor and coatings industries. Recent advancements in ToF-SIMS instrumentation including analyzer design as well as the availability of cluster ion sources have expanded its new applications in the analysis of polymer and biological materials. One major advantage of using the ToF-SIMS technique is its ability to probe simultaneously the localization of several hundred molecules across a sample surface without chemical labels. The recent advances of using the GCIB ion sources make it possible to probe high mass intact lipids with less fragmentation. All of these advantages have brought new exciting applications for ToF-SIMS use to a wide range of fields, especially biological and medical science.

The work done in this thesis demonstrates the application of ToF-SIMS imaging for lipidomic investigations in biological model systems treated with drugs like cocaine, MPH, and zinc deficient diet. This technique provides insights into the chemical actions of the drugs as well as lipid changes at the cellular level. One major advantage of using ToF-SIMS for biological science is its ability to collect simultaneously chemical and spatial information of several lipid species on the sample surface. The information obtained from ToF-SIMS images provides a view of the alteration of biomolecules occurring after various drug treatments. The ToF-SIMS approach provides a better understanding of the role of lipids in cognitive performance. It is clearly possible that the lipid changes observed are associated with the cognition deficits caused by some drugs. This opens up new opportunities for drug development and therapies for impairment of cognitive function.

In addition to the study of lipid changes induced by drugs, ToF-SIMS shows promise for the detection and tracking of biomolecules by using stable

isotopically labelled compounds. In this work, lipid synthesis was investigated by tracking the incorporation of the deuterium isotope labelled omega-3 and -6 fatty acids in the plasma membrane of cells. The combination of ToF-SIMS and stable isotope labelling has established the opportunity to determine and relatively quantify biomolecules at the subcellular level. The identification of possible cellular metabolism might again provide a new target for the development of drugs.

To summarize, in this thesis, ToF-SIMS imaging has been used to probe chemical structure as well as monitor lipid changes in biological materials of both fly brains and single neuronal-like cells. ToF-SIMS also offers a complementary approach for other analysis methods to answer more complicated scientific questions.

Acknowledgements

My PhD has been one of the greatest challenges of my life, it has been a journey filled with joy, excitement, difficulties and much frustration. I count myself very lucky to have people around me that are willing to help me overcome the aforementioned difficulties and give me the support that I needed.

First of all, I would like to thank my supervisor **Andy Ewing**, who gave me the chance to work in his research group as a PhD student. You always provided me with expertise, excellent guidance and encouragement throughout my research and hopefully beyond my stay at Chalmers. You taught me how to write a proper paper and how to present my research in a clear and concise way. It has been a great honor and privilege to study and work under your supervision.

To my co-supervisor, **Per Malmberg**, thank you for teaching me about the ION.TOF 5 and helping me to carry out the research as well as giving me all the support throughout the years.

I would also like to thank Professor **John Fletcher** for all the help with J105, for all of his great advices, comments and the discussions we have had.

To **Nhu Phan**, without you my stay in Gothenburg would not have been the same. You have introduced me to so many new friends. I am really grateful for all the guidance and help you have given through the years.

To all my co-authors, **Nhu Phan, Sanna Sämfors, and Chaoyi**, thank you so much for the cooperation and for giving me the time and effort.

To **Kelly and Chaoyi**, my officemates, thank you for all the nice chats and scientific discussions we had in our office. We all shared the sweet stuffs, especially candies and cookies.

References

(1) Fischbach, G. D. (1992) Mind and Brain. *Sci Am* **267** (3), 48-57.

(2) Zuber, B., Nikonenko, I., Klauser, P., Muller, D., and Dubochet, J. (2005) The mammalian central nervous synaptic cleft contains a high density of periodically organized complexes. *Proc Natl Acad Sci U S A* **102** (52), 19192-19197.

(3) De-Miguel, F. F., and Nicholls, J. G. (2015) Release of chemical transmitters from cell bodies and dendrites of nerve cells. *Philos Trans R Soc Lond B Biol Sci* **370** (1672), 20140181.

(4) Li, S., Wong, A. H., and Liu, F. (2014) Ligand-gated ion channel interacting proteins and their role in neuroprotection. *Front Cell Neurosci* **8**, 125.

(5) Rosenbaum, D. M., Rasmussen, S. G., and Kobilka, B. K. (2009) The structure and function of G-protein-coupled receptors. *Nature* **459** (7245), 356-363.

(6) Klenchin, V. A., and Martin, T. F. (2000) Priming in exocytosis: attaining fusion-competence after vesicle docking. *Biochimie* **82** (5), 399-407.

(7) Matos, M. F., Mukherjee, K., Chen, X., Rizo, J., and Sudhof, T. C. (2003) Evidence for SNARE zippering during Ca2+-triggered exocytosis in PC12 cells. *Neuropharmacology* **45** (6), 777-786.

(8) Del Castillo, J., and Katz, B. (1954) Quantal components of the end-plate potential. *J Physiol* **124** (3), 560-573.

(9) Amatore, C., Oleinick, A. I., and Svir, I. (2010) Reconstruction of aperture functions during full fusion in vesicular exocytosis of neurotransmitters. *Chemphyschem* **11** (1), 159-174.

(10) Omiatek, D. M., Dong, Y., Heien, M. L., and Ewing, A. G. (2010) Only a Fraction of Quantal Content is Released During Exocytosis as Revealed by Electrochemical Cytometry of Secretory Vesicles. *ACS Chem Neurosci* **1** (3), 234-245.

(11) Ren, L., Mellander, L. J., Keighron, J., Cans, A. S., Kurczy, M. E., Svir, I., Oleinick, A., Amatore, C., and Ewing, A. G. (2016) The evidence for open and closed exocytosis as the primary release mechanism. *Q Rev Biophys* **49**, e12.

(12) dela Pena, I., Gevorkiana, R., and Shi, W. X. (2015) Psychostimulants affect dopamine transmission through both dopamine transporter-dependent and independent mechanisms. *Eur J Pharmacol* **764**, 562-570.

(13) Sulzer, D., Sonders, M. S., Poulsen, N. W., and Galli, A. (2005) Mechanisms of neurotransmitter release by amphetamines: a review. *Prog Neurobiol* **75** (6), 406-433.

(14) Kitamura, O. (2009) Detection of methamphetamine neurotoxicity in forensic autopsy cases. *Leg Med (Tokyo)* **11 Suppl 1**, S63-S65.

(15) Nobili, A., Latagliata, E. C., Viscomi, M. T., Cavallucci, V., Cutuli, D., Giacovazzo, G., Krashia, P., Rizzo, F. R., Marino, R., Federici, M., De Bartolo, P., Aversa, D., Dell'Acqua, M. C., Cordella, A., Sancandi, M., Keller, F., Petrosini, L., Puglisi-Allegra, S., Mercuri, N. B., Coccurello, R., Berretta, N., and D'Amelio, M. (2017) Dopamine neuronal loss contributes to memory and reward dysfunction in a model of Alzheimer's disease. *Nat Commun* **8**, 14727.

(16) Masato, A., Plotegher, N., Boassa, D., and Bubacco, L. (2019) Impaired dopamine metabolism in Parkinson's disease pathogenesis. *Mol Neurodegener* **14** (1), 35.

(17) Wood, S., Sage, J. R., Shuman, T., and Anagnostaras, S. G. (2014) Psychostimulants and cognition: a continuum of behavioral and cognitive activation. *Pharmacol Rev* **66** (1), 193-221.

(18) Penner, R., and Neher, E. (1989) The patch-clamp technique in the study of secretion. *Trends Neurosci* **12** (4), 159-163.

(19) Matthews, G. (1996) Synaptic exocytosis and endocytosis: capacitance measurements. *Curr Opin Neurobiol* **6** (3), 358-364.

(20) Leszczyszyn, D. J., Jankowski, J. A., Viveros, O. H., Diliberto, E. J., Jr., Near, J. A., and Wightman, R. M. (1990) Nicotinic receptor-mediated catecholamine secretion from individual chromaffin cells. Chemical evidence for exocytosis. *J Biol Chem* **265** (25), 14736-14737.

(21) Wightman, R. M., Jankowski, J. A., Kennedy, R. T., Kawagoe, K. T., Schroeder, T. J., Leszczyszyn, D. J., Near, J. A., Diliberto, E. J., Jr., and Viveros, O. H. (1991) Temporally resolved catecholamine spikes correspond to single vesicle release from individual chromaffin cells. *Proc Natl Acad Sci U S A* **88** (23), 10754-10758.

(22) Albillos, A., Dernick, G., Horstmann, H., Almers, W., Alvarez de Toledo, G., and Lindau, M. (1997) The exocytotic event in chromaffin cells revealed by patch amperometry. *Nature* **389** (6650), 509-512.

(23) Omiatek, D. M., Cans, A. S., Heien, M. L., and Ewing, A. G. (2010) Analytical approaches to investigate transmitter content and release from single secretory vesicles. *Anal Bioanal Chem* **397** (8), 3269-3279.

(24) Betz, W. J., Mao, F., and Bewick, G. S. (1992) Activity-dependent fluorescent staining and destaining of living vertebrate motor nerve terminals. *J Neurosci* **12** (2), 363-375.

(25) Stevens, C. F., and Williams, J. H. (2000) "Kiss and run" exocytosis at hippocampal synapses. *Proc Natl Acad Sci U S A* **97** (23), 12828-12833.

(26) Gubernator, N. G., Zhang, H., Staal, R. G., Mosharov, E. V., Pereira, D. B., Yue, M., Balsanek, V., Vadola, P. A., Mukherjee, B., Edwards, R. H., Sulzer, D., and Sames, D. (2009) Fluorescent false neurotransmitters visualize dopamine release from individual presynaptic terminals. *Science* **324** (5933), 1441-1444.

(27) Lee, M., Gubernator, N. G., Sulzer, D., and Sames, D. (2010) Development of pH-responsive fluorescent false neurotransmitters. *J Am Chem Soc* **132** (26), 8828-8830.

(28) Rodriguez, P. C., Pereira, D. B., Borgkvist, A., Wong, M. Y., Barnard, C., Sonders, M. S., Zhang, H., Sames, D., and Sulzer, D. (2013) Fluorescent dopamine tracer resolves individual dopaminergic synapses and their activity in the brain. *P Natl Acad Sci USA* **110** (3), 870-875.

(29) Wang, C., Kong, H., Guan, Y., Yang, J., Gu, J., Yang, S., and Xu, G. (2005) Plasma phospholipid metabolic profiling and biomarkers of type 2 diabetes mellitus based on high-performance liquid chromatography/electrospray mass spectrometry and multivariate statistical analysis. *Anal Chem* **77** (13), 4108-4116.

(30) Menendez, J. A., and Lupu, R. (2007) Fatty acid synthase and the lipogenic phenotype in cancer pathogenesis. *Nat Rev Cancer* **7** (10), 763-777.

(31) Kaya, I., Zetterberg, H., Blennow, K., and Hanrieder, J. (2018) Shedding Light on the Molecular Pathology of Amyloid Plaques in Transgenic Alzheimer's Disease Mice Using Multimodal MALDI Imaging Mass Spectrometry. *ACS Chem Neurosci* **9** (7), 1802-1817.

(32) Shi, Y. (2010) Emerging roles of cardiolipin remodeling in mitochondrial dysfunction associated with diabetes, obesity, and cardiovascular diseases. *J Biomed Res* **24** (1), 6-15.

(33) Fahy, E., Cotter, D., Sud, M., and Subramaniam, S. (2011) Lipid classification, structures and tools. *Biochim Biophys Acta* **1811** (11), 637-647.

(34) Riezman, H. (2007) The long and short of fatty acid synthesis. *Cell* **130** (4), 587-588.

(35) Nakamura, M. T., and Nara, T. Y. (2004) Structure, function, and dietary regulation of delta6, delta5, and delta9 desaturases. *Annu Rev Nutr* **24**, 345-376.

(36) Tauchi-Sato, K., Ozeki, S., Houjou, T., Taguchi, R., and Fujimoto, T. (2002) The surface of lipid droplets is a phospholipid monolayer with a unique Fatty Acid composition. *J Biol Chem* **277** (46), 44507-44512.

(37) Mackay, H. J., and Twelves, C. J. (2007) Targeting the protein kinase C family: are we there yet? *Nat Rev Cancer* **7** (7), 554-562.

(38) Carrasco, S., and Merida, I. (2007) Diacylglycerol, when simplicity becomes complex. *Trends Biochem Sci* **32** (1), 27-36.

(39) Fagone, P., and Jackowski, S. (2009) Membrane phospholipid synthesis and endoplasmic reticulum function. *J Lipid Res* **50 Suppl**, S311-S316.

(40) Vance, J. E. (2014) MAM (mitochondria-associated membranes) in mammalian cells: lipids and beyond. *Biochim Biophys Acta* **1841** (4), 595-609.

(41) Wang, X., Devaiah, S. P., Zhang, W., and Welti, R. (2006) Signaling functions of phosphatidic acid. *Prog Lipid Res* **45** (3), 250-278.

(42) Ammar, M. R., Kassas, N., Bader, M. F., and Vitale, N. (2014) Phosphatidic acid in neuronal development: a node for membrane and cytoskeleton rearrangements. *Biochimie* **107 Pt A**, 51-57.

(43) Kennedy, E. P., and Weiss, S. B. (1956) The function of cytidine coenzymes in the biosynthesis of phospholipides. *J Biol Chem* **222** (1), 193-214.

(44) Vance, D. E., and Ridgway, N. D. (1988) The methylation of phosphatidylethanolamine. *Prog Lipid Res* **27** (1), 61-79.

(45) Vance, J. E., and Tasseva, G. (2013) Formation and function of phosphatidylserine and phosphatidylethanolamine in mammalian cells. *Biochim Biophys Acta* **1831** (3), 543-554.

(46) Borkenhagen, L., Kennedy, E. P., and Fielding, L. (1961) Enzymatic Formation and Decarboxylation of Phosphatidylserine. *Journal of Biological Chemistry* **236** (6), Pc28.

(47) Stone, S. J., and Vance, J. E. (2000) Phosphatidylserine synthase-1 and -2 are localized to mitochondria-associated membranes. *J Biol Chem* **275** (44), 34534-34540.

(48) Fischl, A. S., and Carman, G. M. (1983) Phosphatidylinositol biosynthesis in Saccharomyces cerevisiae: purification and properties of microsome-associated phosphatidylinositol synthase. *J Bacteriol* **154** (1), 304-311.

(49) Wenk, M. R., Lucast, L., Di Paolo, G., Romanelli, A. J., Suchy, S. F., Nussbaum, R. L., Cline, G. W., Shulman, G. I., McMurray, W., and De Camilli, P. (2003) Phosphoinositide profiling in complex lipid mixtures using electrospray ionization mass spectrometry. *Nat Biotechnol* **21** (7), 813-817.

(50) Falkenburger, B. H., Jensen, J. B., Dickson, E. J., Suh, B. C., and Hille, B. (2010) Phosphoinositides: lipid regulators of membrane proteins. *J Physiol* **588** (Pt 17), 3179-3185.

(51) Martin, T. F. (2015) PI(4,5)P(2)-binding effector proteins for vesicle exocytosis. *Biochim Biophys Acta* **1851** (6), 785-793.

(52) Kim, H. Y., Huang, B. X., and Spector, A. A. (2014) Phosphatidylserine in the brain: metabolism and function. *Prog Lipid Res* **56**, 1-18.

(53) Horvath, S. E., and Daum, G. (2013) Lipids of mitochondria. *Prog Lipid Res* **52** (4), 590-614.

(54) Schagger, H. (2002) Respiratory chain supercomplexes of mitochondria and bacteria. *Biochim Biophys Acta* **1555** (1-3), 154-159.

(55) Zhang, M., Mileykovskaya, E., and Dowhan, W. (2002) Gluing the respiratory chain together. Cardiolipin is required for supercomplex formation in the inner mitochondrial membrane. *J Biol Chem* **277** (46), 43553-43556.

(56) Sparagna, G. C., Chicco, A. J., Murphy, R. C., Bristow, M. R., Johnson, C. A., Rees, M. L., Maxey, M. L., McCune, S. A., and Moore, R. L. (2007) Loss of cardiac tetralinoleoyl cardiolipin in human and experimental heart failure. *J Lipid Res* **48** (7), 1559-1570.

(57) Steward, C. G., Newbury-Ecob, R. A., Hastings, R., Smithson, S. F., Tsai-Goodman, B., Quarrell, O. W., Kulik, W., Wanders, R., Pennock, M., Williams, M., Cresswell, J. L., Gonzalez, I. L., and Brennan, P. (2010) Barth syndrome: an X-linked cause of fetal cardiomyopathy and stillbirth. *Prenat Diagn* **30** (10), 970-976.

(58) Bartke, N., and Hannun, Y. A. (2009) Bioactive sphingolipids: metabolism and function. *J Lipid Res* **50 Suppl**, S91-S96.

(59) Kolesnick, R. (2002) The therapeutic potential of modulating the ceramide/sphingomyelin pathway. *J Clin Invest* **110** (1), 3-8.

(60) Pettus, B. J., Chalfant, C. E., and Hannun, Y. A. (2002) Ceramide in apoptosis: an overview and current perspectives. *Biochim Biophys Acta* **1585** (2-3), 114-125.

(61) Massey, J. B. (2001) Interaction of ceramides with phosphatidylcholine, sphingomyelin and sphingomyelin/cholesterol bilayers. *Biochim Biophys Acta* **1510** (1-2), 167-184.

(62) Veldman, R. J., Maestre, N., Aduib, O. M., Medin, J. A., Salvayre, R., and Levade, T. (2001) A neutral sphingomyelinase resides in sphingolipid-enriched microdomains and is inhibited by the caveolin-scaffolding domain: potential implications in tumour necrosis factor signalling. *Biochem J* **355** (Pt 3), 859-868.

(63) Draelos, Z. D. (2008) The effect of ceramide-containing skin care products on eczema resolution duration. *Cutis* **81** (1), 87-91.

(64) Huitema, K., van den Dikkenberg, J., Brouwers, J. F., and Holthuis, J. C. (2004) Identification of a family of animal sphingomyelin synthases. *EMBO J* **23** (1), 33-44.

(65) Simons, K., and Toomre, D. (2000) Lipid rafts and signal transduction. *Nat Rev Mol Cell Biol* **1** (1), 31-39.

(66) Engelman, J. A., Luo, J., and Cantley, L. C. (2006) The evolution of phosphatidylinositol 3-kinases as regulators of growth and metabolism. *Nat Rev Genet* **7** (8), 606-619.

(67) Taha, T. A., Mullen, T. D., and Obeid, L. M. (2006) A house divided: ceramide, sphingosine, and sphingosine-1-phosphate in programmed cell death. *Biochim Biophys Acta* **1758** (12), 2027-2036.

(68) Rosen, H., and Goetzl, E. J. (2005) Sphingosine 1-phosphate and its receptors: an autocrine and paracrine network. *Nat Rev Immunol* **5** (7), 560-570.

(69) Lang, T., Halemani, N. D., and Rammner, B. (2008) Interplay between lipids and the proteinaceous membrane fusion machinery. *Prog Lipid Res* **47** (6), 461-469.

(70) Lauwers, E., Goodchild, R., and Verstreken, P. (2016) Membrane Lipids in Presynaptic Function and Disease. *Neuron* **90** (1), 11-25.

(71) Chasserot-Golaz, S., Coorssen, J. R., Meunier, F. A., and Vitale, N. (2010) Lipid dynamics in exocytosis. *Cell Mol Neurobiol* **30** (8), 1335-1342.

(72) McMahon, H. T., and Boucrot, E. (2015) Membrane curvature at a glance. *J Cell Sci* **128** (6), 1065-1070.

(73) Cummings, B. S., Pati, S., Sahin, S., Scholpa, N. E., Monian, P., Trinquero, P. M., Clark, J. K., and Wagner, J. J. (2015) Differential effects of cocaine exposure on the abundance of phospholipid species in rat brain and blood. *Drug Alcohol Depend* **152**, 147-156.

(74) Philipsen, M. H., Phan, N. T. N., Fletcher, J. S., Malmberg, P., and Ewing, A. G. (2018) Mass Spectrometry Imaging Shows Cocaine and Methylphenidate Have Opposite Effects on Major Lipids in Drosophila Brain. *ACS Chem Neurosci* **9** (6), 1462-1468.

(75) Leskawa, K. C., Jackson, G. H., Moody, C. A., and Spear, L. P. (1994) Cocaine exposure during pregnancy affects rat neonate and maternal brain glycosphingolipids. *Brain Res Bull* **33** (2), 195-198.

(76) Haselhorst, U., Ghidoni, R., and Schenk, H. (1991) Changes of brain gangliosides in the frontal cortex of rats chronically treated with amphetamine, clozapine, haloperidol and ethanol. *Biomed Biochim Acta* **50** (7), 931-935.

(77) Bodzon-Kulakowska, A., Antolak, A., Drabik, A., Marszalek-Grabska, M., Kotlinska, J., and Suder, P. (2017) Brain lipidomic changes after morphine, cocaine and amphetamine administration - DESI - MS imaging study. *Biochim Biophys Acta Mol Cell Biol Lipids* **1862** (7), 686-691.

(78) Thomson, J. J. (1897) XL. Cathode rays. *Philos Mag* **44** (269), 293-316.

(79) Aston, F. W. (1919) A positive ray spectrograph. *Philos Mag* **38** (228), 707-714.

(80) Aston, F. W. (1942) Mass spectra and isotopes. *Esward Arnold & Co., London, UK.*

(81) Nier, A. O., and Gulbransen, E. A. (1939) Variations in the relative abundance of the carbon isotopes. *Journal of the American Chemical Society* **61**, 697-698.

(82) Nier, A. O. (1940) A mass spectrometer for routine isotope abundance measurements. *Rev Sci Instrum* **11** (7), 212-216.

(83) Cameron, A. E., and Eggers, D. F. (1948) An Ion Velocitron. *Rev Sci Instrum* **19** (9), 605-607.

(84) Comisarow, M. B., and Marshall, A. G. (1974) Frequency-Sweep Fourier-Transform Ion-Cyclotron Resonance Spectroscopy. *Chem Phys Lett* **26** (4), 489-490.

(85) Herzog, R. F. K., and Viehbock, F. P. (1949) Ion Source for Mass Spectrography. *Phys Rev* **76** (6), 855-856.

(86) Liebl, H. (1967) Ion Microprobe Mass Analyzer. *J Appl Phys* **38** (13), 5277-5283.

(87) Benninghoven, A. (1970) Analysis of Monomolecular Layers of Solids by Secondary Ion Emission. *Z Phys* **230** (5), 403-417.

(88) Pacholski, M. L., and Winograd, N. (1999) Imaging with mass spectrometry. *Chem Rev* **99** (10), 2977-3006.

(89) Davies, N., Weibel, D. E., Blenkinsopp, P., Lockyer, N., Hill, R., and Vickerman, J. C. (2003) Development and experimental application of a gold liquid metal ion source. *Appl Surf Sci* **203**, 223-227.

(90) Kollmer, F. (2004) Cluster primary ion bombardment of organic materials. *Appl Surf Sci* **231**, 153-158.

(91) Mahoney, C. M., Roberson, S. V., and Gillen, G. (2004) Depth profiling of 4-acetamindophenol-doped poly(lactic acid) films using cluster secondary ion mass spectrometry. *Analytical Chemistry* **76** (11), 3199-3207.

(92) Wong, S. C. C., Hill, R., Blenkinsopp, P., Lockyer, N. P., Weibel, D. E., and Vickerman, J. C. (2003) Development of a C-60(+) ion gun for static SIMS and chemical imaging. *Appl Surf Sci* **203**, 219-222.

(93) Nygren, H., and Malmberg, P. (2007) High resolution imaging by organic secondary ion mass spectrometry. *Trends Biotechnol* **25** (11), 499-504.

(94) Ninomiya, S., Ichiki, K., Yamada, H., Nakata, Y., Seki, T., Aoki, T., and Matsuo, J. (2009) Precise and fast secondary ion mass spectrometry depth profiling of polymer materials with large Ar cluster ion beams. *Rapid Commun Mass Spectrom* **23** (11), 1601-1606.

(95) Rabbani, S., Barber, A. M., Fletcher, J. S., Lockyer, N. P., and Vickerman, J. C. (2011) TOF-SIMS with argon gas cluster ion beams: a comparison with C60+. *Anal Chem* **83** (10), 3793-3800.

(96) Chughtai, K., and Heeren, R. M. (2010) Mass spectrometric imaging for biomedical tissue analysis. *Chem Rev* **110** (5), 3237-3277.

(97) Weaver, E. M., and Hummon, A. B. (2013) Imaging mass spectrometry: from tissue sections to cell cultures. *Adv Drug Deliv Rev* **65** (8), 1039-1055.

(98) Rompp, A., and Spengler, B. (2013) Mass spectrometry imaging with high resolution in mass and space. *Histochem Cell Biol* **139** (6), 759-783.

(99) Castaing, R., and Slodzian, G. (1962) Optique Corpusculaire - Premiers Essais De Microanalyse Par Emission Ionique Secondaire. *J. Microscopie* **255** (1), 395-410.

(100) Caprioli, R. M., Farmer, T. B., and Gile, J. (1997) Molecular imaging of biological samples: localization of peptides and proteins using MALDI-TOF MS. *Anal Chem* **69** (23), 4751-4760.

(101) Sigmund, P. (1981) Sputtering by ion bombardment: Theoretical concepts. in *Topics in Applied Physics*. **47**, 9-71.

(102) Matsunami, N., Yamamura, Y., Itikawa, Y., Itoh, N., Kazumata, Y., Miyagawa, S., Morita, K., Shimizu, R., and Tawara, H. (1984) Energy-Dependence of the Ion-Induced Sputtering Yields of Monatomic Solids. *Atom Data Nucl Data* **31** (1), 1-80.

(103) Vickerman, J. C., and Briggs, D. (2013) ToF-SIMS: Material analysis by mass spectrometry. *2nd edition*.

(104) Cheng, J., and Winograd, N. (2005) Depth profiling of peptide films with TOF-SIMS and a C60 probe. *Anal Chem* **77** (11), 3651-3659.

(105) Angerer, T. B., Blenkinsopp, P., and Fletcher, J. S. (2015) High energy gas cluster ions for organic and biological analysis by time-of-flight secondary ion mass spectrometry. *Int J Mass Spectrom* **377**, 591-598.

(106) Hill, R., Blenkinsopp, P., Thompson, S., Vickerman, J., and Fletcher, J. S. (2011) A new time-of-flight SIMS instrument for 3D imaging and analysis. *Surf Interface Anal* **43** (1-2), 506-509.

(107) Rabbani, S., Barber, A. M., Fletcher, J. S., Lockyer, N. P., and Vickerman, J. C. (2011) TOF-SIMS with Argon Gas Cluster Ion Beams: A Comparison with C-60(+). *Analytical Chemistry* **83** (10), 3793-3800.

(108) Wucher, A., Tian, H., and Winograd, N. (2014) A mixed cluster ion beam to enhance the ionization efficiency in molecular secondary ion mass spectrometry. *Rapid Commun Mass Sp* **28** (4), 396-400.

(109) Williams, P. (1982) On Mechanisms of Sputtered Ion Emission. *Appl Surf Sc* **13** (1-2), 241-259.

(110) Sroubek, Z. (1989) Formation of Ions in Sputtering. *Spectrochim Acta B* **44** (3), 317-328.

(111) Wucher, A. (2008) Formation of atomic secondary ions in sputtering. *Appl Surf Sci* **255** (4), 1194-1200.

(112) Wittmaack, K. (2013) Unravelling the secrets of Cs controlled secondary ion formation: Evidence of the dominance of site specific surface chemistry, alloying and ionic bonding. *Surf Sci Rep* **68** (1), 108-230.

(113) Conlan, X. A., Lockyer, N. P., and Vickerman, J. C. (2006) Is proton cationization promoted by polyatomic primary ion bombardment during time-of-flight secondary ion mass spectrometry analysis of frozen aqueous solutions? *Rapid Commun Mass Sp* **20** (8), 1327-1334.

(114) Samfors, S., Ewing, A. G., and Fletcher, J. S. (2018) Benefits of NaCl addition for time-of-flight secondary ion mass spectrometry analysis including the discrimination of diacylglyceride and triacylglyceride ions. *Rapid Commun Mass Sp* **32** (17), 1473-1480.

(115) Tian, H., Wucher, A., and Winograd, N. (2016) Dynamic Reactive Ionization with Cluster Secondary Ion Mass Spectrometry. *J Am Soc Mass Spectr* **27** (2), 285-292.

(116) Sheraz, S., Barber, A., Fletcher, J. S., Lockyer, N. P., and Vickerman, J. C. (2013) Enhancing Secondary Ion Yields in Time of Flight-Secondary Ion Mass Spectrometry Using Water Cluster Primary Beams. *Analytical Chemistry* **85** (12), 5654-5658.

(117) F. Hillion, B. D., F. Girard, and G. Slodzian (1993) A new high performance instrument: the Cameca Nanosims 50. In Secondary Ion Mass Spectrometry: SIMS IX. *Proceedings of the SIMS International conference*, 254–257.

(118) Stadermann, F. J., Walker, R. M., and Zinner, E. (1999) Nanosims: The next generation ion probe for the microanalysis of extraterrestrial material. *Meteorit Planet Sci* **34**, A111-A112.

(119) Lovric, J., Dunevall, J., Larsson, A., Ren, L., Andersson, S., Meibom, A., Malmberg, P., Kurczy, M. E., and Ewing, A. G. (2017) Nano Secondary Ion Mass Spectrometry Imaging of Dopamine Distribution Across Nanometer Vesicles. *ACS Nano* **11** (4), 3446-3455.

(120) Frisz, J. F., Klitzing, H. A., Lou, K., Hutcheon, I. D., Weber, P. K., Zimmerberg, J., and Kraft, M. L. (2013) Sphingolipid domains in the plasma membranes of fibroblasts are not enriched with cholesterol. *J Biol Chem* **288** (23), 16855-16861.

(121) Lee, R. F. S., Theiner, S., Meibom, A., Koellensperger, G., Keppler, B. K., and Dyson, P. J. (2017) Application of imaging mass spectrometry approaches to facilitate metal-based anticancer drug research. *Metallomics* **9** (4), 365-381.

(122) Romer, W., Wu, T. D., Duchambon, P., Amessou, M., Carrez, D., Johannes, L., and Guerquin-Kern, J. L. (2006) Sub-cellular localisation of a N-15-labelled peptide vector using NanoSIMS imaging. *Appl Surf Sci* **252** (19), 6925-6930.

(123) Kleinfeld, A. M., Kampf, J. P., and Lechene, C. (2004) Transport of C-13-oleate in adipocytes measured using multi imaging mass Spectrometry. *J Am Soc Mass Spectr* **15** (11), 1572-1580.

(124) Kraft, M. L., Fishel, S. F., Marxer, C. G., Weber, P. K., Hutcheon, I. D., and Boxer, S. G. (2006) Quantitative analysis of supported membrane composition using the NanoSIMS. *Appl Surf Sci* **252** (19), 6950-6956.

(125) Benninghoven, A., Rudenauer, F.G., and Werner, H.W. (1987) Secondary Ion Mass Spectrometry: Basic Concepts, Instrumental Aspects, Applications and Trends. *Wiley, New York, 1987.*

(126) Agui-Gonzalez, P., Jahne, S., and Phan, N. T. N. (2019) SIMS imaging in neurobiology and cell biology. *J Anal Atom Spectrom* **34** (7), 1355-1368.

(127) Cannon, D. M., Jr., Winograd, N., and Ewing, A. G. (2000) Quantitative chemical analysis of single cells. *Annu Rev Biophys Biomol Struct* **29**, 239-263.

(128) Reichlmaier, S., Hammond, J. S., Hearn, M. J., and Briggs, D. (1994) Analysis of Polymer Surfaces by Sims-17 - an Assessment of the Accuracy of the Mass Assignment Using a High-Mass Resolution Tof-Sims Instrument. *Surf Interface Anal* **21** (11), 739-746.

(129) Benninghoven, A. (1969) Analysis of Submonolayers on Silver by Negative Secondary Ion Emission. *Phys Status Solidi* **34** (2), K169-K171.

(130) Hagenhoff, B. (2000) High resolution surface analysis by TOF-SIMS. *Mikrochim Acta* **132** (2-4), 259-271.

(131) Tian, H., Sparvero, L. J., Amoscato, A. A., Bloom, A., Bayir, H., Kagan, V. E., and Winograd, N. (2017) Gas Cluster Ion Beam Time-of-Flight Secondary

Ion Mass Spectrometry High-Resolution Imaging of Cardiolipin Speciation in the Brain: Identification of Molecular Losses after Traumatic Injury. *Analytical Chemistry* **89** (8), 4611-4619.

(132) Benguerba, M., Brunelle, A., Dellanegra, S., Depauw, J., Joret, H., Lebeyec, Y., Blain, M. G., Schweikert, E. A., Benassayag, G., and Sudraud, P. (1991) Impact of Slow Gold Clusters on Various Solids - Nonlinear Effects in Secondary Ion Emission. *Nucl Instrum Meth B* **62** (1), 8-22.

(133) Smiley, E. J., Winograd, N., and Garrison, B. J. (2007) Effect of cluster size in kiloelectronvolt cluster bombardment of solid benzene. *Analytical Chemistry* **79** (2), 494-499.

(134) Fletcher, J. S., Conlan, X. A., Jones, E. A., Biddulph, G., Lockyer, N. P., and Vickerman, J. C. (2006) TOF-SIMS analysis using C-60- effect of impact energy on yield and damage. *Analytical Chemistry* **78** (6), 1827-1831.

(135) Walker, A. V. (2008) Why Is SIMS Underused in Chemical and Biological Analysis? Challenges and Opportunities. *Analytical Chemistry* **80** (23), 8865-8870.

(136) Fletcher, J. S., Lockyer, N. P., Vaidyanathan, S., and Vickerman, J. C. (2007) TOF-SIMS 3D biomolecular imaging of Xenopus laevis oocytes using buckminsterfullerene (C-60) primary ions. *Analytical Chemistry* **79** (6), 2199-2206.

(137) Jones, E. A., Lockyer, N. P., and Vickerman, J. C. (2007) Mass spectral analysis and imaging of tissue by ToF-SIMS - The role of buckminsterfullerene, C-60(+), primary ions. *Int J Mass Spectrom* **260** (2-3), 146-157.

(138) Bailey, J., Havelund, R., Shard, A. G., Gilmore, I. S., Alexander, M. R., Sharp, J. S., and Scurr, D. J. (2015) 3D ToF-SIMS imaging of polymer multilayer films using argon cluster sputter depth profiling. *ACS Appl Mater Interfaces* **7** (4), 2654-2659.

(139) De Hoffmann, E., and Stroobant, V. (2007) Mass spectrometry: principles and applications. *John Wiley & Sons*.

(140) Mamyrin, B. A., Karataev, V. I., Shmikk, D. V., and Zagulin, V. A. (1973) Mass-Reflectron a New Nonmagnetic Time-of-Flight High-Resolution Mass-Spectrometer. *Zh Eksp Teor Fiz+* **64** (1), 82-89.

(141) Cornish, T. J., and Cotter, R. J. (1995) Non-linear field reflectron. *U.S. Patent* **5** (464), 985.

(142) Fletcher, J. S., Rabbani, S., Henderson, A., Blenkinsopp, P., Thompson, S. P., Lockyer, N. P., and Vickerman, J. C. (2008) A New Dynamic in Mass Spectral Imaging of Single Biological Cells. *Analytical Chemistry* **80** (23), 9058-9064.

(143) Fletcher, J. S. (2009) Cellular imaging with secondary ion mass spectrometry. *Analyst* **134** (11), 2204-2215.

(144) Trouillon, R., Passarelli, M. K., Wang, J., Kurczy, M. E., and Ewing, A. G. (2013) Chemical Analysis of Single Cells. *Analytical Chemistry* **85** (2), 522-542.

(145) Colliver, T. L., Brummel, C. L., Pacholski, M. L., Swanek, F. D., Ewing, A. G., and Winograd, N. (1997) Atomic and molecular imaging at the single-cell level with TOF-SIMS. *Analytical Chemistry* **69** (13), 2225-2231.

(146) Ostrowski, S. G., Van Bell, C. T., Winograd, N., and Ewing, A. G. (2004) Mass spectrometric imaging of highly curved membranes during Tetrahymena mating. *Science* **305** (5680), 71-73.

(147) Kollmer, F., Paul, W., Krehl, M., and Niehuis, E. (2013) Ultra high spatial resolution SIMS with cluster ions - approaching the physical limits. *Surf Interface Anal* **45** (1), 312-314.

(148) Matsuo, J., Okubo, C., Seki, T., Aoki, T., Toyoda, N., and Yamada, I. (2004) A new secondary ion mass spectrometry (SIMS) system with high-intensity cluster ion source. *Nucl Instrum Meth B* **219**, 463-467.

(149) Jones, E. A., Fletcher, J. S., Thompson, C. E., Jackson, D. A., Lockyer, N. P., and Vickerman, J. C. (2006) ToF-SIMS analysis of bio-systems: Are polyatomic primary ions the solution? *Appl Surf Sci* **252** (19), 6844-6854.

(150) Brison, J., Benoit, D. S. W., Muramoto, S., Robinson, M., Stayton, P. S., and Castner, D. G. (2011) ToF-SIMS imaging and depth profiling of HeLa cells treated with bromodeoxyuridine. *Surf Interface Anal* **43** (1-2), 354-357.

(151) Sjovall, P., Lausmaa, J., and Johansson, B. (2004) Mass spectrometric imaging of lipids in brain tissue. *Analytical Chemistry* **76** (15), 4271-4278.

(152) Magnusson, Y., Friberg, P., Sjovall, P., Dangardt, F., Malmberg, P., and Chen, Y. (2008) Lipid imaging of human skeletal muscle using TOF-SIMS with bismuth cluster ion as a primary ion source. *Clin Physiol Funct I* **28** (3), 202-209.

(153) Phan, N. T., Fletcher, J. S., and Ewing, A. G. (2015) Lipid structural effects of oral administration of methylphenidate in Drosophila brain by secondary ion mass spectrometry imaging. *Anal Chem* **87** (8), 4063-4071.

(154) Skraskova, K., Khmelinskii, A., Abdelmoula, W. M., De Munter, S., Baes, M., McDonnell, L., Dijkstra, J., and Heeren, R. M. A. (2015) Precise Anatomic Localization of Accumulated Lipids in Mfp2 Deficient Murine Brains Through Automated Registration of SIMS Images to the Allen Brain Atlas. *J Am Soc Mass Spectr* **26** (6), 948-957.

(155) Vanbellingen, Q. P., Elie, N., Eller, M. J., Della-Negra, S., Touboul, D., and Brunelle, A. (2015) Time-of-flight secondary ion mass spectrometry imaging

of biological samples with delayed extraction for high mass and high spatial resolutions. *Rapid Commun Mass Sp* **29** (13), 1187-1195.

(156) Philipsen, M. H., Samfors, S., Malmberg, P., and Ewing, A. G. (2018) Relative quantification of deuterated omega-3 and-6 fatty acids and their lipid turnover in PC12 cell membranes using TOF-SIMS. *Journal of Lipid Research* **59** (11), 2098-2107.

(157) Samfors, S., Stahlman, M., Klevstig, M., Boren, J., and Fletcher, J. S. (2019) Localised lipid accumulation detected in infarcted mouse heart tissue using ToF-SIMS. *Int J Mass Spectrom* **437**, 77-86.

(158) Lazar, A. N., Bich, C., Panchal, M., Desbenoit, N., Petit, V. W., Touboul, D., Dauphinot, L., Marquer, C., Laprevote, O., Brunelle, A., and Duyckaerts, C. (2013) Time-of-flight secondary ion mass spectrometry (TOF-SIMS) imaging reveals cholesterol overload in the cerebral cortex of Alzheimer disease patients. *Acta Neuropathologica* **125** (1), 133-144.

(159) Ide, Y., Waki, M., Ishizaki, I., Nagata, Y., Yamazaki, F., Hayasaka, T., Masaki, N., Ikegami, K., Kondo, T., Shibata, K., Ogura, H., Sanada, N., and Setou, M. (2014) Single cell lipidomics of SKBR-3 breast cancer cells by using time-of-flight secondary-ion mass spectrometry. *Surf Interface Anal* **46**, 181-184.

(160) Angerer, T. B., Magnusson, Y., Landberg, G., and Fletcher, J. S. (2016) Lipid Heterogeneity Resulting from Fatty Acid Processing in the Human Breast Cancer Microenvironment Identified by GCIB-ToF-SIMS Imaging. *Analytical Chemistry* **88** (23), 11946-11954.

(161) Lazar, A. N., Bich, C., Panchal, M., Desbenoit, N., Petit, V. W., Touboul, D., Dauphinot, L., Marquer, C., Laprevote, O., Brunelle, A., and Duyckaerts, C. (2013) Time-of-flight secondary ion mass spectrometry (TOF-SIMS) imaging reveals cholesterol overload in the cerebral cortex of Alzheimer disease patients. *Acta Neuropathol* **125** (1), 133-144.

(162) Piwowar, A., Fletcher, J., Lockyer, N., and Vickerman, J. (2011) Investigating the effect of temperature on depth profiles of biological material using ToF-SIMS. *Surf Interface Anal* **43** (1-2), 207-210.

(163) Dimovska Nilsson, K., Palm, M., Hood, J., Sheriff, J., Farewell, A., and Fletcher, J. S. (2019) Chemical Changes On, and Through, The Bacterial Envelope in Escherichia coli Mutants Exhibiting Impaired Plasmid Transfer Identified Using Time-of-Flight Secondary Ion Mass Spectrometry. *Analytical Chemistry* **91** (17), 11355-11361.

(164) Rubakhin, S. S., Greenough, W. T., and Sweedler, J. V. (2003) Spatial profiling with MALDI MS: distribution of neuropeptides within single neurons. *Anal Chem* **75** (20), 5374-5380.

(165) Agar, N. Y., Yang, H. W., Carroll, R. S., Black, P. M., and Agar, J. N. (2007) Matrix solution fixation: histology-compatible tissue preparation for MALDI mass spectrometry imaging. *Anal Chem* **79** (19), 7416-7423.

(166) Stoeckli, M., Staab, D., Schweitzer, A., Gardiner, J., and Seebach, D. (2007) Imaging of a beta-peptide distribution in whole-body mice sections by MALDI mass spectrometry. *J Am Soc Mass Spectrom* **18** (11), 1921-1924.

(167) Pierson, J., Norris, J. L., Aerni, H. R., Svenningsson, P., Caprioli, R. M., and Andren, P. E. (2004) Molecular profiling of experimental Parkinson's disease: direct analysis of peptides and proteins on brain tissue sections by MALDI mass spectrometry. *J Proteome Res* **3** (2), 289-295.

(168) Patel, R. (2015) MALDI-TOF MS for the diagnosis of infectious diseases. *Clin Chem* **61** (1), 100-111.

(169) Sjovall, P., Lausmaa, J., Nygren, H., Carlsson, L., and Malmberg, P. (2003) Imaging of membrane lipids in single cells by imprint-imaging time-of-flight secondary ion mass spectrometry. *Analytical Chemistry* **75** (14), 3429-3434.

(170) Takats, Z., Wiseman, J. M., Gologan, B., and Cooks, R. G. (2004) Mass spectrometry sampling under ambient conditions with desorption electrospray ionization. *Science* **306** (5695), 471-473.

(171) Wiseman, J. M., Ifa, D. R., Song, Q., and Cooks, R. G. (2006) Tissue imaging at atmospheric pressure using desorption electrospray ionization (DESI) mass spectrometry. *Angew Chem Int Ed Engl* **45** (43), 7188-7192.

(172) Venter, A., Sojka, P. E., and Cooks, R. G. (2006) Droplet dynamics and ionization mechanisms in desorption electrospray ionization mass spectrometry. *Anal Chem* **78** (24), 8549-8555.

(173) Marshall, A. G., Hendrickson, C. L., and Jackson, G. S. (1998) Fourier transform ion cyclotron resonance mass spectrometry: a primer. *Mass Spectrom Rev* **17** (1), 1-35.

(174) Smith, D. F., Robinson, E. W., Tolmachev, A. V., Heeren, R. M., and Pasa-Tolic, L. (2011) C60 secondary ion Fourier transform ion cyclotron resonance mass spectrometry. *Anal Chem* **83** (24), 9552-6.

(175) Passarelli, M. K., Pirkl, A., Moellers, R., Grinfeld, D., Kollmer, F., Havelund, R., Newman, C. F., Marshall, P. S., Arlinghaus, H., Alexander, M. R., West, A., Horning, S., Niehuis, E., Makarov, A., Dollery, C. T., and Gilmore, I.

S. (2017) The 3D OrbiSIMS-label-free metabolic imaging with subcellular lateral resolution and high mass-resolving power. *Nat Methods* **14** (12), 1175-1183.

(176) Adams, M. D., Celniker, S. E., Holt, R. A., Evans, C. A., Gocayne, J. D., Amanatides, P. G., Scherer, S. E., Li, P. W., Hoskins, R. A., Galle, R. F., George, R. A., Lewis, S. E., Richards, S., Ashburner, M., Henderson, S. N., Sutton, G. G., Wortman, J. R., Yandell, M. D., Zhang, Q., Chen, L. X., Brandon, R. C., Rogers, Y. H., Blazej, R. G., Champe, M., Pfeiffer, B. D., Wan, K. H., Doyle, C., Baxter, E. G., Helt, G., Nelson, C. R., Gabor, G. L., Abril, J. F., Agbayani, A., An, H. J., Andrews-Pfannkoch, C., Baldwin, D., Ballew, R. M., Basu, A., Baxendale, J., Bayraktaroglu, L., Beasley, E. M., Beeson, K. Y., Benos, P. V., Berman, B. P., Bhandari, D., Bolshakov, S., Borkova, D., Botchan, M. R., Bouck, J., Brokstein, P., Brottier, P., Burtis, K. C., Busam, D. A., Butler, H., Cadieu, E., Center, A., Chandra, I., Cherry, J. M., Cawley, S., Dahlke, C., Davenport, L. B., Davies, P., de Pablos, B., Delcher, A., Deng, Z., Mays, A. D., Dew, I., Dietz, S. M., Dodson, K., Doup, L. E., Downes, M., Dugan-Rocha, S., Dunkov, B. C., Dunn, P., Durbin, K. J., Evangelista, C. C., Ferraz, C., Ferriera, S., Fleischmann, W., Fosler, C., Gabrielian, A. E., Garg, N. S., Gelbart, W. M., Glasser, K., Glodek, A., Gong, F., Gorrell, J. H., Gu, Z., Guan, P., Harris, M., Harris, N. L., Harvey, D., Heiman, T. J., Hernandez, J. R., Houck, J., Hostin, D., Houston, K. A., Howland, T. J., Wei, M. H., Ibegwam, C., Jalali, M., Kalush, F., Karpen, G. H., Ke, Z., Kennison, J. A., Ketchum, K. A., Kimmel, B. E., Kodira, C. D., Kraft, C., Kravitz, S., Kulp, D., Lai, Z., Lasko, P., Lei, Y., Levitsky, A. A., Li, J., Li, Z., Liang, Y., Lin, X., Liu, X., Mattei, B., McIntosh, T. C., McLeod, M. P., McPherson, D., Merkulov, G., Milshina, N. V., Mobarry, C., Morris, J., Moshrefi, A., Mount, S. M., Moy, M., Murphy, B., Murphy, L., Muzny, D. M., Nelson, D. L., Nelson, D. R., Nelson, K. A., Nixon, K., Nusskern, D. R., Pacleb, J. M., Palazzolo, M., Pittman, G. S., Pan, S., Pollard, J., Puri, V., Reese, M. G., Reinert, K., Remington, K., Saunders, R. D., Scheeler, F., Shen, H., Shue, B. C., Siden-Kiamos, I., Simpson, M., Skupski, M. P., Smith, T., Spier, E., Spradling, A. C., Stapleton, M., Strong, R., Sun, E., Svirskas, R., Tector, C., Turner, R., Venter, E., Wang, A. H., Wang, X., Wang, Z. Y., Wassarman, D. A., Weinstock, G. M., Weissenbach, J., Williams, S. M., WoodageT, Worley, K. C., Wu, D., Yang, S., Yao, Q. A., Ye, J., Yeh, R. F., Zaveri, J. S., Zhan, M., Zhang, G., Zhao, Q., Zheng, L., Zheng, X. H., Zhong, F. N., Zhong, W., Zhou, X., Zhu, S., Zhu, X., Smith, H. O., Gibbs, R. A., Myers, E. W., Rubin, G. M., and Venter, J. C. (2000) The genome sequence of Drosophila melanogaster. *Science* **287** (5461), 2185-2195.

(177) Reiter, L. T., Potocki, L., Chien, S., Gribskov, M., and Bier, E. (2001) A systematic analysis of human disease-associated gene sequences in Drosophila melanogaster. *Genome Res* **11** (6), 1114-1125.

(178) Bonini, N. M., and Fortini, M. E. (2002) Applications of the Drosophila retina to human disease modeling. *Results Probl Cell Differ* **37**, 257-275.

(179) Iijima, K., Liu, H. P., Chiang, A. S., Hearn, S. A., Konsolaki, M., and Zhong, Y. (2004) Dissecting the pathological effects of human Abeta40 and Abeta42 in Drosophila: a potential model for Alzheimer's disease. *Proc Natl Acad Sci U S A* **101** (17), 6623-6628.

(180) Iijima, K., and Iijima-Ando, K. (2008) Drosophila models of Alzheimer's amyloidosis: the challenge of dissecting the complex mechanisms of toxicity of amyloid-beta 42. *J Alzheimers Dis* **15** (4), 523-540.

(181) Piazza, N., and Wessells, R. J. (2011) Drosophila models of cardiac disease. *Prog Mol Biol Transl Sci* **100**, 155-210.

(182) Guo, M. (2012) Drosophila as a model to study mitochondrial dysfunction in Parkinson's disease. *Cold Spring Harb Perspect Med* **2** (11), a009944.

(183) Bellen, H. J., Tong, C., and Tsuda, H. (2010) 100 years of Drosophila research and its impact on vertebrate neuroscience: a history lesson for the future. *Nat Rev Neurosci* **11** (7), 514-522.

(184) Ong, C., Yung, L. Y., Cai, Y., Bay, B. H., and Baeg, G. H. (2015) Drosophila melanogaster as a model organism to study nanotoxicity. *Nanotoxicology* **9** (3), 396-403.

(185) Gordon, M. D., Manzo, A., and Scott, K. (2008) Fly neurobiology: development and function of the brain. Meeting on the Neurobiology of Drosophila. *EMBO Rep* **9** (3), 239-242.

(186) Scott, K., Brady, R., Jr., Cravchik, A., Morozov, P., Rzhetsky, A., Zuker, C., and Axel, R. (2001) A chemosensory gene family encoding candidate gustatory and olfactory receptors in Drosophila. *Cell* **104** (5), 661-673.

(187) Herculano-Houzel, S. (2009) The human brain in numbers: a linearly scaled-up primate brain. *Front Hum Neurosci* **3**, 1-31.

(188) Chiang, A. S., Lin, C. Y., Chuang, C. C., Chang, H. M., Hsieh, C. H., Yeh, C. W., Shih, C. T., Wu, J. J., Wang, G. T., Chen, Y. C., Wu, C. C., Chen, G. Y., Ching, Y. T., Lee, P. C., Lin, C. Y., Lin, H. H., Wu, C. C., Hsu, H. W., Huang, Y. A., Chen, J. Y., Chiang, H. J., Lu, C. F., Ni, R. F., Yeh, C. Y., and Hwang, J. K. (2011) Three-dimensional reconstruction of brain-wide wiring networks in Drosophila at single-cell resolution. *Curr Biol* **21** (1), 1-11.

(189) Yasuyama, K., Kitamoto, T., and Salvaterra, P. M. (1995) Localization of choline acetyltransferase-expressing neurons in the larval visual system of Drosophila melanogaster. *Cell Tissue Res* **282** (2), 193-202.

(190) Daniels, R. W., Gelfand, M. V., Collins, C. A., and DiAntonio, A. (2008) Visualizing glutamatergic cell bodies and synapses in Drosophila larval and adult CNS. *J Comp Neurol* **508** (1), 131-152.

(191) Denno, M. E., Privman, E., and Venton, B. J. (2015) Analysis of neurotransmitter tissue content of Drosophila melanogaster in different life stages. *ACS Chem Neurosci* **6** (1), 117-123.

(192) Majdi, S., Berglund, E. C., Dunevall, J., Oleinick, A. I., Amatore, C., Krantz, D. E., and Ewing, A. G. (2015) Electrochemical Measurements of Optogenetically Stimulated Quantal Amine Release from Single Nerve Cell Varicosities in Drosophila Larvae. *Angew Chem Int Ed Engl* **54** (46), 13609-13612.

(193) Pollack, I., and Hofbauer, A. (1991) Histamine-like immunoreactivity in the visual system and brain of Drosophila melanogaster. *Cell Tissue Res* **266** (2), 391-398.

(194) Makos, M. A., Kim, Y. C., Han, K. A., Heien, M. L., and Ewing, A. G. (2009) In vivo electrochemical measurements of exogenously applied dopamine in Drosophila melanogaster. *Anal Chem* **81** (5), 1848-1854.

(195) Berglund, E. C., Makos, M. A., Keighron, J. D., Phan, N., Heien, M. L., and Ewing, A. G. (2013) Oral administration of methylphenidate blocks the effect of cocaine on uptake at the Drosophila dopamine transporter. *ACS Chem Neurosci* **4** (4), 566-574.

(196) Liu, Z., and Huang, X. (2013) Lipid metabolism in Drosophila: development and disease. *Acta Biochim Biophys Sin (Shanghai)* **45** (1), 44-50.

(197) Greene, L. A., and Tischler, A. S. (1976) Establishment of a noradrenergic clonal line of rat adrenal pheochromocytoma cells which respond to nerve growth factor. *Proc Natl Acad Sci U S A* **73** (7), 2424-2428.

(198) Chen, T. K., Luo, G., and Ewing, A. G. (1994) Amperometric monitoring of stimulated catecholamine release from rat pheochromocytoma (PC12) cells at the zeptomole level. *Anal Chem* **66** (19), 3031-3035.

(199) Westerink, R. H., and Ewing, A. G. (2008) The PC12 cell as model for neurosecretion. *Acta Physiol* **192** (2), 273-285.

(200) Huang, E. J., and Reichardt, L. F. (2001) Neurotrophins: roles in neuronal development and function. *Annu Rev Neurosci* **24**, 677-736.

(201) Greene, L. A., and Rein, G. (1977) Release, storage and uptake of catecholamines by a clonal cell line of nerve growth factor (NGF) responsive pheo-chromocytoma cells. *Brain Res* **129** (2), 247-263.

(202) Travis, E. R., and Wightman, R. M. (1998) Spatio-temporal resolution of exocytosis from individual cells. *Annu Rev Biophys Biomol Struct* **27**, 77-103.

(203) Zerby, S. E., and Ewing, A. G. (1996) Electrochemical monitoring of individual exocytotic events from the varicosities of differentiated PC12 cells. *Brain Res* **712** (1), 1-10.

(204) Wang, X., Xu, Y., Song, X., Jia, Q., Zhang, X., Qian, Y., and Qiu, J. (2019) Analysis of glycerophospholipid metabolism after exposure to PCB153 in PC12 cells through targeted lipidomics by UHPLC-MS/MS. *Ecotoxicol Environ Saf* **169**, 120-127.

(205) Najafinobar, N., Mellander, L. J., Kurczy, M. E., Dunevall, J., Angerer, T. B., Fletcher, J. S., and Cans, A. S. (2016) Cholesterol Alters the Dynamics of Release in Protein Independent Cell Models for Exocytosis. *Sci Rep* **6**, 33702.

(206) Corsetto, P. A., Ferrara, G., Buratta, S., Urbanelli, L., Montorfano, G., Gambelunghe, A., Chiaradia, E., Magini, A., Roderi, P., Colombo, I., Rizzo, A. M., and Emiliani, C. (2016) Changes in Lipid Composition During Manganese-Induced Apoptosis in PC12 Cells. *Neurochem Res* **41** (1-2), 258-269.

(207) Yoon, S., and Lee, T. G. (2018) Biological tissue sample preparation for time-of-flight secondary ion mass spectrometry (ToF-SIMS) imaging. *Nano Converg* **5**, 24.

(208) Berman, E. S. F., Fortson, S. L., Checchi, K. D., Wu, L., Felton, J. S., Wu, K. J. J., and Kulp, K. S. (2008) Preparation of single cells for imaging/profiling mass spectrometry. *J Am Soc Mass Spectr* **19** (8), 1230-1236.

(209) Sjovall, P., Johansson, B., and Lausmaa, J. (2006) Localization of lipids in freeze-dried mouse brain sections by imaging TOF-SIMS. *Appl Surf Sci* **252** (19), 6966-6974.

(210) Bich, C., Havelund, R., Moellers, R., Touboul, D., Kollmer, F., Niehuis, E., Gilmore, I. S., and Brunelle, A. (2013) Argon Cluster Ion Source Evaluation on Lipid Standards and Rat Brain Tissue Samples. *Analytical Chemistry* **85** (16), 7745-7752.

(211) Phan, N. T. N., Fletcher, J. S., Sjovall, P., and Ewing, A. G. (2014) ToF-SIMS imaging of lipids and lipid related compounds in Drosophila brain. *Surf Interface Anal* **46**, 123-126.

(212) Chandra, S., Bernius, M. T., and Morrison, G. H. (1986) Intracellular-Localization of Diffusible Elements in Frozen-Hydrated Biological Specimens with Ion Microscopy. *Analytical Chemistry* **58** (2), 493-496.

(213) Chandra, S. (2008) Challenges of biological sample preparation for SIMS imaging of elements and molecules at subcellular resolution. *Appl Surf Sci* **255** (4), 1273-1284.

(214) Fletcher, J. S., Rabbani, S., Henderson, A., Lockyer, N. P., and Vickerman, J. C. (2011) Three-dimensional mass spectral imaging of HeLa-M cells - sample preparation, data interpretation and visualisation. *Rapid Commun Mass Sp* **25** (7), 925-932.

(215) Kurczy, M. E., Piehowski, P. D., Parry, S. A., Jiang, M., Chen, G., Ewing, A. G., and Winograd, N. (2008) Which is more important in bioimaging SIMS experiments-The sample preparation or the nature of the projectile? *Appl Surf Sci* **255** (4), 1298-1304.

(216) Cannon, D. M., Pacholski, M. L., Winograd, N., and Ewing, A. G. (2000) Molecule specific imaging of freeze-fractured, frozen-hydrated model membrane systems using mass spectrometry. *Journal of the American Chemical Society* **122** (4), 603-610.

(217) Lanekoff, I., Kurczy, M. E., Hill, R., Fletcher, J. S., Vickerman, J. C., Winograd, N., Sjovall, P., and Ewing, A. G. (2010) Time of Flight Mass Spectrometry Imaging of Samples Fractured In Situ with a Spring-Loaded Trap System. *Analytical Chemistry* **82** (15), 6652-6659.

(218) Malm, J., Giannaras, D., Riehle, M. O., Gadegaard, N., and Sjovall, P. (2009) Fixation and Drying Protocols for the Preparation of Cell Samples for Time-of-Flight Secondary Ion Mass Spectrometry Analysis. *Analytical Chemistry* **81** (17), 7197-7205.

(219) Kraft, M. L., and Klitzing, H. A. (2014) Imaging lipids with secondary ion mass spectrometry. *Biochim Biophys Acta* **1841** (8), 1108-1119.

(220) Altelaar, A. F., van Minnen, J., Jimenez, C. R., Heeren, R. M., and Piersma, S. R. (2005) Direct molecular imaging of Lymnaea stagnalis nervous tissue at subcellular spatial resolution by mass spectrometry. *Anal Chem* **77** (3), 735-741.

(221) Adriaensen, L., Vangaever, F., and Gijbels, R. (2004) Metal-assisted secondary ion mass spectrometry: influence of Ag and Au deposition on molecular ion yields. *Anal Chem* **76** (22), 6777-6785.

(222) Angerer, T. B., Dowlatshahi Pour, M., Malmberg, P., and Fletcher, J. S. (2015) Improved molecular imaging in rodent brain with time-of-flight-

secondary ion mass spectrometry using gas cluster ion beams and reactive vapor exposure. *Anal Chem* **87** (8), 4305-4313.

(223) Angerer, T. B., Mohammadi, A. S., and Fletcher, J. S. (2016) Optimizing sample preparation for anatomical determination in the hippocampus of rodent brain by ToF-SIMS analysis. *Biointerphases* **11** (2), 02A319.

(224) Vaidyanathan, S., Fletcher, J. S., Henderson, A., Lockyer, N. P., and Vickerman, J. C. (2008) Exploratory analysis of TOF-SIMS data from biological surfaces. *Appl Surf Sci* **255** (4), 1599-1602.

(225) Vaidyanathan, S., Fletcher, J. S., Jarvis, R. M., Henderson, A., Lockyer, N. P., Goodacre, R., and Vickerman, J. C. (2009) Explanatory multivariate analysis of ToF-SIMS spectra for the discrimination of bacterial isolates. *Analyst* **134** (11), 2352-2360.

(226) Tyler, B. J., Rayal, G., and Castner, D. G. (2007) Multivariate analysis strategies for processing ToF-SIMS images of biomaterials. *Biomaterials* **28** (15), 2412-2423.

(227) Graham, D. J., and Castner, D. G. (2012) Multivariate analysis of ToF-SIMS data from multicomponent systems: the why, when, and how. *Biointerphases* **7** (1-4), 49.